Development of Mouse Hepatocyte Lines Permissive for Hepatitis C Virus (HCV)

Hussein Hassan Aly[1], Hiroyuki Oshiumi[1], Hiroaki Shime[1], Misako Matsumoto[1], Taka Wakita[2], Kunitada Shimotohno[3], Tsukasa Seya[1]*

1 Department of Microbiology and Immunology, Hokkaido University Graduate School of Medicine, Sapporo, Hokkaido, Japan, **2** Department of Virology II, National Institute of Infectious Diseases, Shinjuku, Tokyo, Japan, **3** Research Institute, Chiba Institute of Technology, Narashino, Chiba, Japan

Abstract

The lack of a suitable small animal model for the analysis of hepatitis C virus (HCV) infection has hampered elucidation of the HCV life cycle and the development of both protective and therapeutic strategies against HCV infection. Human and mouse harbor a comparable system for antiviral type I interferon (IFN) induction and amplification, which regulates viral infection and replication. Using hepatocytes from knockout (ko) mice, we determined the critical step of the IFN-inducing/amplification pathways regulating HCV replication in mouse. The results infer that interferon-beta promoter stimulator (IPS-1) or interferon A receptor (IFNAR) were a crucial barrier to HCV replication in mouse hepatocytes. Although both IFNARko and IPS-1ko hepatocytes showed a reduced induction of type I interferons in response to viral infection, only IPS-1-/- cells circumvented cell death from HCV cytopathic effect and significantly improved J6JFH1 replication, suggesting IPS-1 to be a key player regulating HCV replication in mouse hepatocytes. We then established mouse hepatocyte lines lacking IPS-1 or IFNAR through immortalization with SV40T antigen. Expression of human (h)CD81 on these hepatocyte lines rendered both lines HCVcc-permissive. We also found that the chimeric J6JFH1 construct, having the structure region from J6 isolate enhanced HCV replication in mouse hepatocytes rather than the full length original JFH1 construct, a new finding that suggests the possible role of the HCV structural region in HCV replication. This is the first report on the entry and replication of HCV infectious particles in mouse hepatocytes. These mouse hepatocyte lines will facilitate establishing a mouse HCV infection model with multifarious applications.

Citation: Aly HH, Oshiumi H, Shime H, Matsumoto M, Wakita T, et al. (2011) Development of Mouse Hepatocyte Lines Permissive for Hepatitis C Virus (HCV). PLoS ONE 6(6): e21284. doi:10.1371/journal.pone.0021284

Editor: Jacques Zimmer, Centre de Recherche Public de la Santé (CRP-Santé), Luxembourg

Received May 13, 2011; **Accepted** May 24, 2011; **Published** June 22, 2011

Funding: This work was supported in part by Grants-in-Aid from the Ministry of Education, Science, and Culture (Specified Project for Advanced Research), the Ministry of Health, Labor, and Welfare of Japan, and the Hokkaido University Leader Development System in the Basic Interdisciplinary Research Areas (L station). Supports from Mitsubishi Foundation, Mochida Foundation, NorthTec Foundation Waxman Foundation and Yakult Foundation are gratefully acknowledged. The funders had no role in study design, data collection and analysis, decision to publish, or preparation of the manuscript.

Competing Interests: The authors have declared that no competing interests exist.

* E-mail: seya-tu@pop.med.hokudai.ac.jp

Introduction

Chronic hepatitis C virus (HCV) infection is a major cause of mortality and morbidity throughout the world infecting around 3.1% of the world's population [1]. The development of much needed specific antiviral therapies and an effective vaccine has been hampered by the lack of a suitable small animal model. The determinants restricting HCV tropism to human and chimpanzee hosts are unknown. Replication of HCV strain JFH1 has been demonstrated in mouse cells only upon antibody selection [2], highlighting the very limited replication efficiency. Human CD81 and occludin have been implicated as important entry receptors for retrovirus particles bearing HCV glycoproteins, HCV pseudoparticles (HCVpp), into NIH3T3 murine cells [3]. However, HCV infection, spontaneous replication and particle production by mouse cells have not yet been reported.

In mammalian cells, the host detects and responds to infection by RNA-viruses, including HCV, by primarily recognizing viral RNA through several distinct pathogen recognition receptors (PRRs), including the cell surface and endosomal RNA sensors Toll-like receptors 3 and 7 (TLR3 and TLR7), and the cytoplasmic RNA sensors retinoic acid-inducible gene I (RIG-I) and melanoma differentiation associated gene 5 (MDA5) [4]. The detection of virus infection by these receptors leads to the induction of interferons (IFNs) and their downstream IFN-inducible anti-viral genes through distinct signaling pathways [5]. Type I IFN is an important regulator of viral infections in the innate immune system [6]. Another type of IFN, IFN-lambda, affects the prognosis of HCV infection, and its response to antiviral therapy [7,8].

Mutations impairing the function of the RIG-I gene and the induction of IFN were essential in establishing HCV infectivity in human HuH7.5 cells [9]. Similarly, the HCV-NS3/4a protease is known to cleave IPS-1 adaptor molecule, inducing further downstream blocking of the IFN-inducing signaling pathway [10]. These data clearly demonstrate that the host RIG-I pathway is crucial for suppressing HCV proliferation in human hepatocytes. Using a similar strategy, we investigated whether suppressing the antiviral host innate immune system conferred any advantage on HCV proliferation in mouse hepatocytes. We examined the possibility of HCV replication in mice lacking the expression of key factors that modulate the type I IFN-inducing pathways. Only gene silencing of the IFN receptor (IFNAR) or IPS-1 was sufficient to establish spontaneous HCV replication in

mouse hepatocytes. To establish a cell line permissive for HCV replication, which is required for further *in vitro* studies of the HCV life cycle in mouse hepatocytes, we immortalized IFNAR- and IPS-1-knockout (ko) mice hepatocytes with SV40 T antigen. Upon expression of the human (h)CD81 gene, these newly established cell lines were able to support HCV infection for the first time in mouse hepatocytes. Viral factors required for HCV replication in mouse hepatocytes were also analyzed.

Results

IPS-1-mediated IFN signaling is important for HCV replication in mouse hepatocytes

As a first step in establishing HCV infection in mice, we tested the susceptibility of mouse hepatocytes to persistent expression of HCV proteins after RNA transfection. *In vitro* transcribed chimeric J6JFH1 RNA, in which the HCV structural and non-structural regions were from J6 and JFH1 isolates respectively, was transfected into hepatocytes from wild-type mice. We used a highly sensitive polyclonal antibody derived from HCV-patient serum for the detection of HCV proteins. No HCV proteins were detected five days after transfection (Fig. 1 A), suggesting that wild-type mouse hepatocytes were unable to maintain HCV replication. We then tried to find and block the pathway used by mouse hepatocytes for the detection of viral-RNA and the induction of IFN response. Mouse hepatocytes did not show the expression of either TLR3 or TLR7 as detected by RT-PCR, unlike IPS-1 and RIG-I which was fairly detected (Fig. S1), suggesting that the cytoplasmic RIG-I/IPS-1 pathway is the main pathway utilized by mouse hepatocytes for the detection of RNA viruses. We then checked the susceptibility of hepatocytes from TICAM-1ko, IPS-1ko and IFNARko mice to the prolonged expression of HCV proteins (Fig. 1B–D). Only IPS-1- and IFNARko mouse hepatocytes showed expression of J6JFH1 proteins five days after transfection (Fig. 1), indicating the importance of impaired IPS-1 and/or IFNAR receptors for HCV persistence. Similarly, the detection of the J6JFH1-RNA in transfected hepatocyte lines from various knockout mice showed higher levels in IPS-1 or IFNAR knockout cells compared to TICAM-1knockout cells in which a rapid decline of J6JFH1-RNA levels was noticed similar to the non-replicating control JFH1GND construct (Fig. S2). These data clearly suggest that the RIG-I/IPS-1 but not TLR3/TICAM-1 is the main pathway utilized for the detection of HCV-RNA and the induction of anti-viral immune response in mouse hepatocytes. Its suppression significantly improves HCV replication in mouse hepatocytes.

Establishment and characterization of immortalized mouse hepatocyte cell lines lacking expression of the IFNAR or IPS-1 gene

We further established mouse hepatocyte lines with disrupted IFNAR or IPS-1 genes through immortalization with SV40T antigen, and used these cell lines to study factors required for the HCV life cycle. Hepatocytes were transduced with SV40T-expressing lentivirus vectors. Six weeks after transduction, hepatocytes transduced with SV40T showed continuous proliferation and clonally proliferating hepatocyte lines were selected. SV40T-immortalized IFNARko and IPS-1ko clones were designated IRK (Fig. 2 A) and IPK (Fig. 2 B), respectively. 20 IRK and 19 IPK clones were picked up, of which IRK clones 2 and 4 (IRK2 and IRK4) and IPK clones 10 and 17 (IPK10 and IPK17) were most closely related to primary mouse hepatocytes in term of differentiation (Fig. 2 C) and were used in the following experiments. Expression of SV40T was confirmed by RT-PCR analysis (data not shown). IRK2, IRK4, IPK10 and IPK17, but not the non-hepatocytic NIH3T3 cells, displayed albumin and hepatocyte nuclear factor 4 (HNF4) expression similar to that observed in liver tissue, but did not express the bile duct marker, cytokeratin. IRK and IPK cells did not show expression of IFNAR and IPS-1 respectively (Fig. 2 C).

Replication of the HCV genome in IRK and IPK cells

To assess the permissiveness of the established cell lines to HCV replication, we transduced IRK4 and IPK17 cells with J6JFH1 RNA and monitored the HCV protein and RNA levels by IF (Fig. 3 A) and real time RT-PCR (Fig. 3 B). The number of cells expressing HCV proteins, as detected by IF, increased over time, indicating the continuous proliferation of J6JFH1 in these cells. However, the ratio between infected and non-infected cells did not significantly change over time for 7 days after transfection. Similarly, the amount of total J6JFH1 RNA in 1 μg of total cellular RNA was reasonably constant. By contrast, the level of

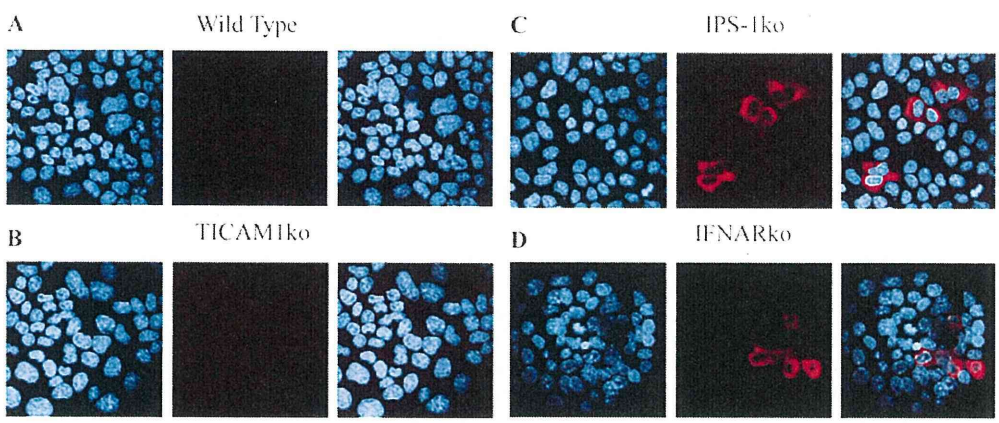

Figure 1. IF detection of of J6JFH1 proteins' expression 5 days after transfection of J6JFH1-RNA through electroporation into wild type (A), TICAM-1ko (B), IPS-1ko (C), and IFNARko (D), freshly isolated primary hepatocytes. A highly sensitive polyclonal antibody extracted from HCV-patient serum (AbS3) was used for the detection. Staining of the uninfected hepatocytes from different Ko mice was also performed and they showed negative for HCV proteins (data not shown).
doi:10.1371/journal.pone.0021284.g001

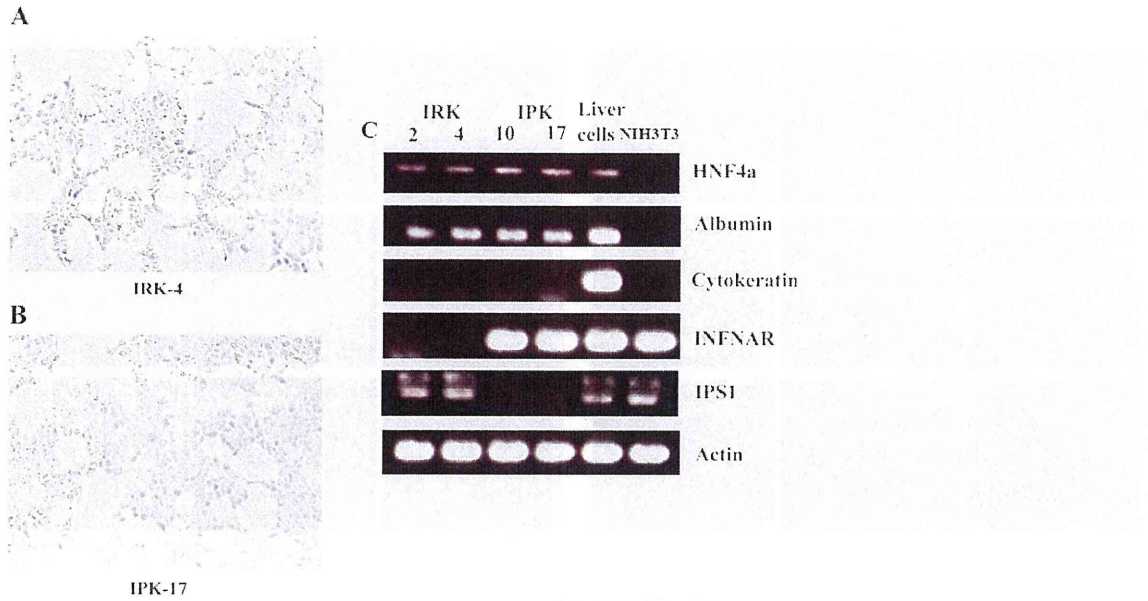

Figure 2. Morphological characteristics of IRK-4 (A) and IPK-17 (B) cells. (C) RT analysis for the expression of albumin, HNF4, cytokeratin, interferon A receptor, and IPS-1 in 2 IFNAR-KO cell lines (IRK2 and 4), 2 IPS-1-KO cell lines (IPK-10 and 17), total liver, and NIH3T3 cells.
doi:10.1371/journal.pone.0021284.g002

JFH1GND RNA carrying a mutation in NS5B hampering HCV replication, rapidly declined, indicating the requirement of continuous HCV replication for the maintenance of HCV positivity in the transfected mouse hepatocytes. Similar data were obtained from IRK2 and IPK10 cells (data not shown).

IPS-1-dependent/Interferon-independent pathway is responsible for HCV's cytopathic effect

In comparison to IPS-1ko hepatocytes, J6JFH1-RNA in IFNARko were lower and decreased further after its transfection, while higher stable levels of J6JFH1-RNA were maintained in IPS-1ko cells (Fig. 3 B and Fig. S2). Similarly, larger numbers of HCV-positive cells were detected in IPS-1ko hepatocytes compared with their IFNARko counterparts (Fig. 3 A), suggesting that the IPS-1 disruption benefits HCV replication in a distinct manner from IFNAR disruption. To measure the interferon induction after RNA virus infection in those cells, we used a highly infectious RNA-Virus (VSV) and measured the induction of interferon after its infection. All the interferons measured showed similar suppression of induction in IFNARko and IPS-1ko hepatocytes (Fig. 4). Surprisingly, cellular cytopathic effect that was monitored after transfection of J6JFH1-RNA was markedly reduced in IPS-1ko but not in IFNARko hepatocytes after transfection (Fig. 5A). This suppression was accompanied by an increase of J6JFH1-RNA levels in IPS-1ko cells, suggesting that minimal cellular damage induced by HCV replication in IPS-1-/- cells led to the improvement of HCV proliferation in mouse hepatocytes (Fig. 5B).Reduction of HCV-induced cellular cytotoxicity (Fig.5C), and improvement of HCV replication (Fig.5D) in wild type, and IFNAR-KO cells were found when we cultured the cells with a pan-caspase inhibitor, zVAD-fmk, 2 days before and after HCV-RNA transfection. We reasoned that the IPS-1 pathway rather than the IFNAR pathway capacitates hepatocytes to induce HCV-derived apoptotic cell death and its disruption resulted in the circumvention of cell death.

Human CD81 is required for HCV infection of mouse hepatocytes

Similar to the primary mouse hepatocytes, immortalized mouse hepatocytes showed the expression of all the mouse counterparts of human HCV entry receptors (Fig. S3). Human CD81 and hOccludin, but not other human HCV receptors such as SR-B1 or claudin1, have previously been reported to be essential for HCVpp entry into NIH3T3 mouse cells [3]. We then expressed hCD81 and/or hOccludin in IRK2 and IRK4 cells using lentivirus vectors. Using a MOI of 10, 95% transfection efficiency was achieved (Fig. S4) with lentivirus vector. We next tested the effect of these proteins on HCV particle (HCVcc) infection. Human CD81 alone was found to be required for J6JFH1 infection into all IRK and IPK cells tested (Fig. S5 and Fig. 6 A, and B). For the first time in mouse hepatocytes, HCV proteins were detected in nearly 1% of the cells used for infection. These data demonstrated the importance of hCD81 in establishing HCVcc infection in mouse hepatocytes.

Viral factors affecting HCV replication in mouse hepatocytes

After successfully establishing J6JFH1 infection in mouse hepatocytes, we attempted to infect these cells with other strains of HCV. Human CD81-expressing IPK17 cells were infected with full-length JFH1FL, however, no infection was detected (data not shown). This might be due to a problem in infection and/or replication. We further examined the replication efficiency of JFH1FL, the subgenomic JFH1 replicon and the J6JFH1 chimera in two different mouse hepatocyte lines and the HuH7.5.1 cell line. The persistent expression of HCV proteins was detected seven days after RNA transfection. Although HCV proteins were detected in HuH7.5.1 cells in all cases (Fig. 7 C), only J6JFH1 proteins were detected in the mouse hepatocyte lines, suggesting for the first time the importance of the J6 structural region for the replication of HCV in mouse hepatocytes (Fig. 7 A, and B).

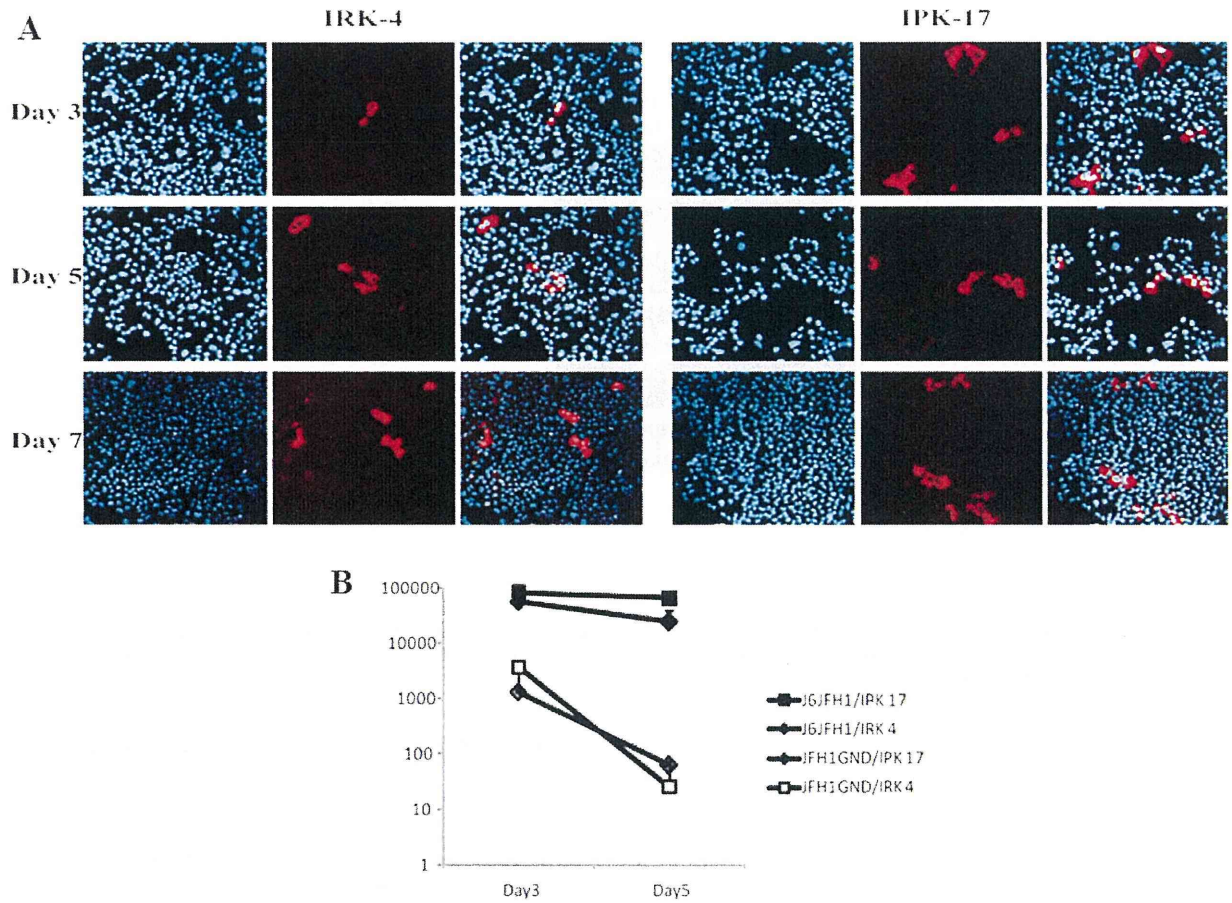

Figure 3. Proliferation of HCV in IRK4 and IPK17 cells over time as detected by immunofluorescence staining of NS5a protein using the CL1 rabbit polyclonal antibody (A) and by quantitative real-time RT-PCR analysis of HCV-RNA levels (B). JFH1GND was used as a negative control to exclude non replicating HCV-RNA. The data plotted represent the average +/− STD of 3 different experiments.
doi:10.1371/journal.pone.0021284.g003

Discussion

Gene silencing of either IPS-1 or IFNAR significantly improves HCV replication and persistence in mouse hepatocytes compared with wild-type or TICAM-1ko mice. This result demonstrated the importance of the IPS-1 pathway rather than the TICAM-1 pathway in the induction of type I IFN by HCV infection, and revealed that the IFNAR amplification pathway confers resistance to HCV in mouse hepatocytes independently of TICAM-1. In accordance with our data, HCV-NS3/4A protease is known to cleave the IPS-1 and/or RIG-I-complement molecules including DDX3 and Riplet in humans to overcome the host innate immune response, showing the importance of RIG-I/IPS-1 pathway suppression in the establishment of HCV infection [10,11,12].

To further study factors affecting the HCV life cycle in mouse hepatocytes, we established IPK and IRK immortalized mouse hepatocyte lines by transduction with SV40T antigen. The established hepatocytes cell lines showed expression of HNF4, a major hepatocyte transcription factor, required for hepatocyte differentiation and liver-specific gene expression [13]. The maintenance of hepatocellular functions was demonstrated by continuous expression of hepatocyte specific differentiation marker, albumin, and the lack of expression of the bile duct marker, cytokeratin. The close resemblance of these cell lines to primary mouse hepatocytes is crucial to ensure the physiological relevance of factors identified in these cell lines that affect the HCV life cycle.

It is worth noting that HCV replication in IPS-1ko was higher than that in IFNARko hepatocytes. Since IPS-1 is present upstream of IFNAR in the IFN-amplification pathway, this higher J6JFH1 replication efficiency in IPS-1ko hepatocytes suggested the presence of an additive factor affecting HCV replication other than the induction of IFNAR-mediated type I IFN. This enhanced replication efficiency was also not accompanied by the induction of other interferon types, but was correlated with the reduction of HCV-induced apoptosis in mouse hepatocytes. This data clearly demonstrates that IPS-1 is playing an important role in the regulation of HCV infection in mouse hepatocytes through two different pathways, the IFN-induction pathways and another new IFN-independent pathway, leading to apoptotic cell death and elimination of HCV-harboring hepatocytes. The cytopathic effect of HCV infection in human cells is still contradictory. Although, some reports showed the induction of apoptosis and cell death by HCV infection in human hepatocytes [14,15,16], others showed suppression of apoptosis by HCV proteins [17,18]. This difference may be due to the different cell lines used in the different studies. Almost all the studies reporting HCV-induced apoptosis used

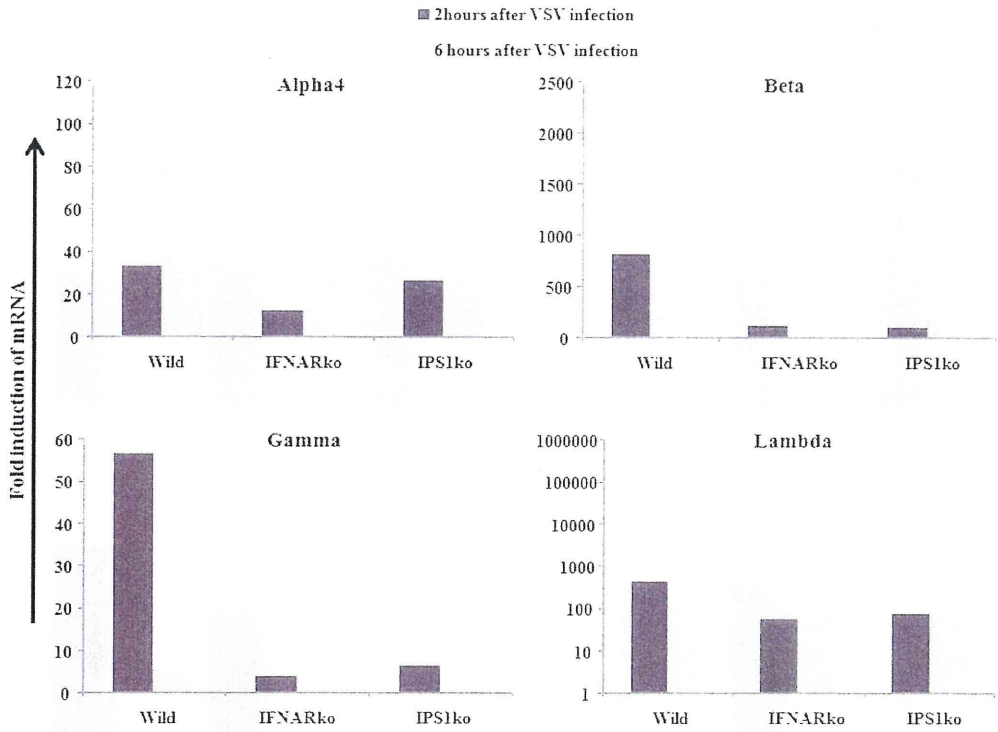

Figure 4. Wild type, IFNARko, and IPS-1ko mice hepatocytes were infected with mock or VSV virus, 2 and 6 hours later, total RNA was extracted from the cells, and interferon alpha, beta, gamma and lambda mRNA induction levels were measured by real-time RT-PCR. Similar results were obtained from 2 different experiments, each was performed in duplicates. The data plotted represent the mean duplicate readings in one of them.
doi:10.1371/journal.pone.0021284.g004

hepatocellular carcinoma cell lines. Since it has been established that the inability to undergo apoptosis is essential for the development of cancer [19,20,21], our use of immortalized, non-cancerous hepatocytes may make it possible to reproduce the physiological response of the cells to HCV infection more closely. The IPS-1 regulation of cell death following the introduction of HCV-RNA may also regulate the effector cell function. It is likely that hepatocyte debris generated secondary to intrinsic production of viral dsRNA in HCV-infected hepatocytes affect the antiviral effector response of the immune system through maturation of dendritic cells [22]. Hence, the effector cell activation may be enhanced by the induction of cell death through the IPS-1 pathway in hepatocytes which may facilitate producing dsRNA-containing debris.

In comparison to the JFH1GND construct with deficient replication that showed a rapid reduction in its RNA levels over time after transfection into mouse hepatocytes, J6JFH1 RNA was detected at four-log higher levels and was maintained at a relatively stable levels in IPS-1ko hepatocytes. Although the number of mouse cells expressing HCV proteins was found to increase over time, as detected by IF, the ratio between HCV-negative and -positive cells did not show any significant change for 7 days after transfection and increased after 10 days (data not shown). This indicates a negative selection of HCV-bearing cells over time which may be due to slower cellular replication, or loss of HCV replication. Another possibility may be that HCV infection is affected by the presence of an inhibitory factor possibly triggered by HCV replication or the lack of a human host factor required for HCV replication. Due to the initial replication of HCV in the transfected IPK and IRK mouse hepatocytes for the first 7 days and the establishment of infection, we favor the presence of a possible inhibitory factor that may be triggered by HCV replication. Another factor that also limits HCV spread in mouse hepatocytes is the failure of HCV to produce infectious particles in these cells (data no shown).

Using this newly established immortalized mouse hepatocyte line, we found that although J6JFH1, JFH1FL and the subgenomic JFH1 replicon all share a similar non-structural region derived from isolate JFH1 that is required for HCV replication, and although all of these constructs can replicate efficiently in HuH7.5.1 cells, strikingly, only J6JFH1 carrying the J6 structural region replicated in mouse hepatocytes. This indicates the importance of the J6 structural region and/or the chimeric construct between J6 and JFH1 for HCV replication in mouse hepatocytes. Structural regions are known to be important for HCV entry and/or particle formation [23], but this is the first time that their importance in replication in HCV-bearing cells has been demonstrated. This finding clearly shows the importance of non-hepatoma cell lines with less genetic abnormalities and mutations for the discovery of new aspects of the life cycle of HCV.

Although, the co-expression of human CD81 and Occludin genes was found to be important for HCVpp entry into murine NIH3T3 cells [3], the expression of hCD81 alone was sufficient for J6JFH1 entry into mouse hepatocytes. This may be explained by the different cell lines used in the different studies. In contrast to NIH3T3 cells, we used immortalized hepatocytes that showed close physiological resemblance to primary mouse hepatocytes and showed the expression of all the mouse counterparts of HCV entry

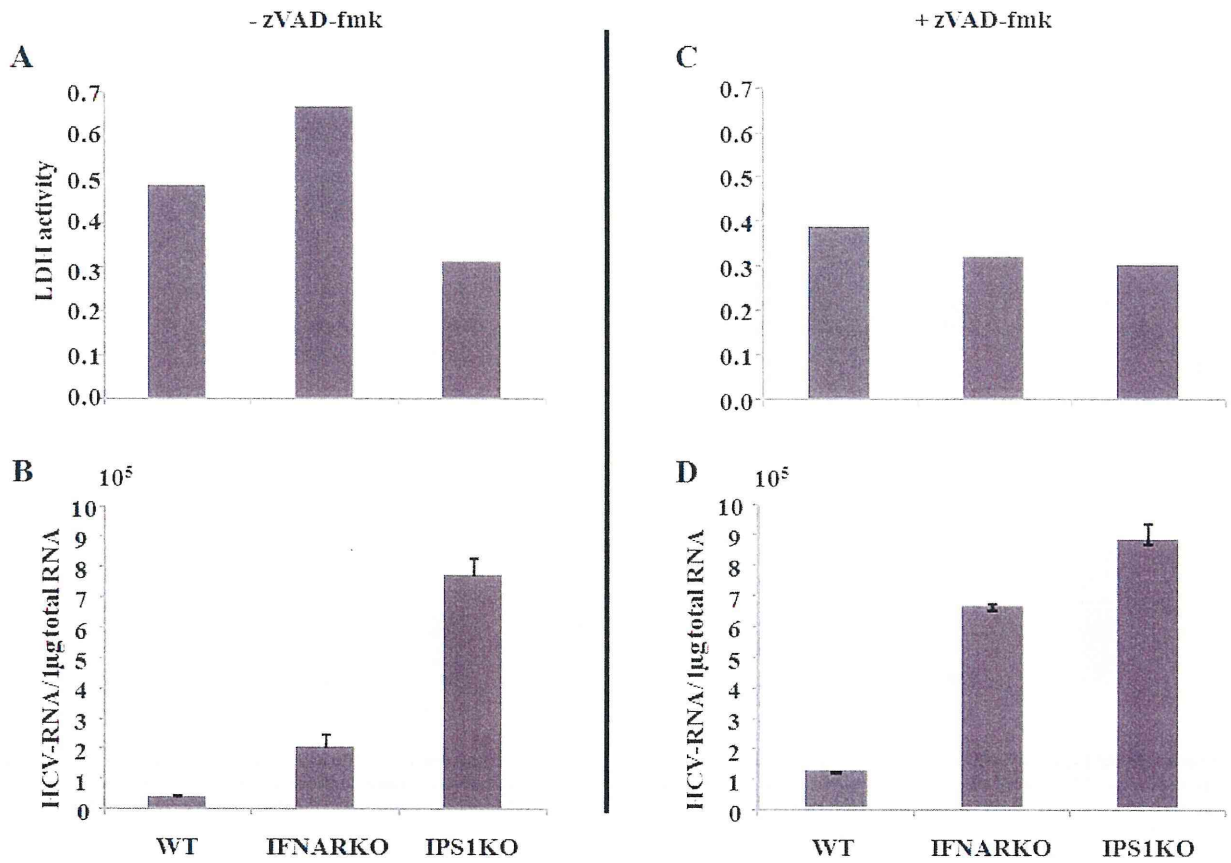

Figure 5. Measurement of J6JFH1 mediated cytopathic effect in wild type, IFNARko, and IPS-1ko mouse hepatocytes. Culture medium were left untreated (A;B) or treated with 20 μM of zVAD-fmK (C;D) 2 days before and after J6JFH1-RNA transfection. One day after transfection of J6JFH1-RNA, culture medium was discarded and cells were washed with PBS. A new medium was added and cells were cultured for another 24 hours. The LDH activity in the culture medium was measured in 2 different experiments in duplicates and showed similar results, the average levels of a duplicate from a single experiment was plotted (A, C). HCV-RNA titers in the cells were also measured using real-time RT-PCR (B, D), the data shown represent the mean +/− STD of 3 different experiments.
doi:10.1371/journal.pone.0021284.g005

receptors. A study from a different group showed that adaptive mutations in HCV envelope proteins allowing its interaction with murine CD81 is enough for efficient HCVpp entry without the expression of any human entry receptors in murine cells [24]. This report, together with ours, suggest that CD81 is the main human host restriction factor for HCV entry, and that overcoming this problem either by HCV adaptation to murine CD81, or the expression of human CD81 in murine hepatocytes is essential for HCV entry. Although our lentivirus transfection efficiency with CD81 was around 95% in IPK and IRK clones, only 1% of the cells were prone to infection with HCVcc. Also, HCVpp showed lower entry levels in those cells compared to HuH7.5.1 cells (Fig. S6). This suggests that hCD81 expression is the minimum and most crucial requirement for HCV entry into mouse hepatocytes. The discovery and expression of other co-receptors facilitating HCV entry in human cells is still required for efficient and robust HCV infection.

In summary, the suppression of IPS-1 is important for the establishment of HCV infection and replication in mouse hepatocytes through the suppression of both interferon induction and interferon independent J6JFH1-induced cytopathic effect. We have established hepatocytes lines from IPS-1 and IFNARko mice that support HCV replication and infection. These cell lines will be very useful in identifying other species restriction factors and viral determinants required for further establishment of a robust and efficient HCV life cycle in mouse hepatocytes. Using those cells, we showed for the first time the importance of HCV structural region for viral replication. IRF3ko mouse embryo fibroblasts (MEFs) were previously shown to support HCV replication more efficiently than wild MEFs [25]. Since the knockout of IPS-1 mainly suppresses signaling in response to virus RNA detection, and maintains an intact IFN response to other stimulants, it may result in minimum interference to adaptive immune responses as compared to IRF3 or IFNARko. Therefore, further development of hCD81-transgenic IPS-1ko mice may serve as a good model for the study of immunological responses against HCV infection. This mouse model can be used as a backbone for any further future models supporting robust HCV infectivity for the study of HCV pathogenesis, propagation and vaccine development.

Material and Methods

Cell culture

HuH7.5.1 cells were cultured in high-glucose Dulbecco's modified Eagle's medium (DMEM; Gibco/Invitrogen, Tokyo, Japan) supplemented with 2 mM L-glutamine, 100 U of penicillin/ml, 100 μg of

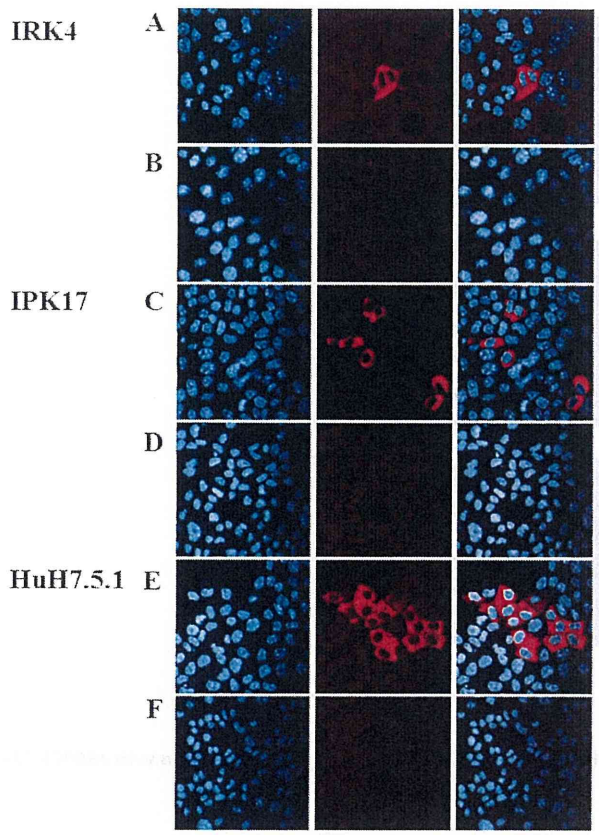

Figure 6. J6JFH1 infection into IRK-4 and IPK17 cells. HCV-NS5A protein detection in mouse IRK4 (A,B) and IPK17 (C,D) and human 7.5.1 cells (E,F). The cells were transduced with lentivirus expressing human CD81 gene at 10 MOI. 48 hours later the cells were infected with 100 times concentrated supernatant medium, collected during 1 week after transfection of HuH7.5.1 cells with J6JFH1-RNA (A, C, and E) or JFH1GND-RNA (B, D, and F).
doi:10.1371/journal.pone.0021284.g006

streptomycin/ml and 10% fetal bovine serum. Mouse primary hepatocytes were isolated from the liver using collagenase perfusion through the inferior vena cava (IVC), while clamping the animal's intrathoracic extension. Hepatocyte isolation and perfusion control were performed as previously described [26]. Primary and immortalized hepatocytes were cultured in a similar medium supplemented with: HEPES (Gibco/Invitrogen), 20 mmol/L; L-proline, 30 μg/mL; insulin (Sigma, St. Louis, MO, USA), 0.5 μg/mL; dexamethasone (Wako, Osaka, Japan), 1×10^{-7} mol/L; $NaHCO_3$, 44 mmol/L; nicotinamide (Wako), 10 mmol/L; EGF (Wako), 10 ng/mL; L-ascorbic acid 2-phosphate (Wako), 0.2 mmol/L; and MEM-non essential amino acids (Gibco/Invitrogen), 1%.

Gene-disrupted mice

All mice were backcrossed with C57BL/6 mice more than seven times before use. Toll-like receptor adaptor molecule 1 (TICAM-1) ko [27] and IPS-1ko mice [28] were generated in our laboratory (detailed information regarding the IPS-1 mice will be presented elsewhere). All mice were maintained under specific-pathogen-free conditions in the animal facility of the Hokkaido University Graduate School of Medicine (Japan).

RNA extraction, reverse transcriptase polymerase chain reaction (RT-PCR) and real-time RT-PCR

RNA was extracted from cultured cells using Trizol reagent (Invitrogen, San Diego, CA, USA) according to the manufacturer's protocol. Using 1 μg of total RNA as a template, we performed RT-PCR and real-time RT-PCR as previously described [29,30].

In vitro RNA transcription, transfection and preparation of J6JFH1 and Jfh1 viruses

In vitro RNA transcription, transfection into HuH7.5.1 or mouse hepatocytes, and preparation of J6JFH1 and JFH1 viruses, were all performed as previously reported [31]. RNA transfection into human and mouse hepatocytes was performed by electroporation using a Gene Pulser II (Bio-Rad, Berkeley, California) at 260 V and 950 Cap.

HCV infection

J6JFH1 and JFH1 concentrated medium were adjusted to contain a similar RNA copy number by real-time RT-PCR. 2×10^4 cells/well were cultured in 8-well glass chamber slides. After 24 hours, the medium was removed and replaced by concentrated medium containing JFH1 or J6JFH1 viruses. After three hours, the concentrated medium was removed, cells were washed with PBS and incubated in fresh medium for 48 hours, before the detection of infection.

Lentivirus construction, titration and infection

The gene encoding T antigen from simian virus was cloned from plasmid CSII-EF-SVT [32]. The genes encoding human CD81 and occludin were cloned from HuH-7.5.1 cells using the Zero Blunt TOPO PCR Cloning Kit (Invitrogen) according to the manufacturer's protocol. These genes were then inserted into the GFP reporter gene-containing lentiviral expression (pLBIG) vector using the *Eco*RI and *Xho*I restriction sites for SV40T and hCD81, and the *Xba*I and *Xho*I restriction sites for hOccludin. Lentivirus expression vectors were then constructed as previously described [27]. GFP expression was used for the titration of lentivirus vectors, and a multiplicity of infection (MOI) of 10 was used for the infection of mouse cells. Forty-eight hours after the transfection of hCD81 and/or hOccludin, cells were trypsinized and counted. Then, 2×10^4 cells/well were cultured in 8-well glass chamber slides for HCV infection and 5×10^4 cells/well were cultured in 12-well plates, along with 1 ml of medium containing HCVpp, for HCV entry experiments.

HCVpp construction and the detection of luciferase expression

HCVpp containing the E1 and E2 proteins from HCV isolate J6 and expressing the luciferase reporter gene were a kind gift from Dr. Thomas Pietschmann at the TWINCORE Center for Experimental and Clinical Infection Research, Germany. The production of HCVpp and the measurement of luciferase levels were performed as previously described [33].

Indirect immunofluorescence (IF)

IF expression of HCV proteins was detected in the infected cells using antibodies in the serum of chronic HCV patients or rabbit IgG anti-NS5A antibody (Cl-1) (both kind gifts from K. Shimotohno, Chiba Institute of Technology, Japan). Goat anti-human IgG Alexa 594 and goat anti-rabbit Alexa 594 (Invitrogen) were used as secondary antibodies, respectively. Fluorescence

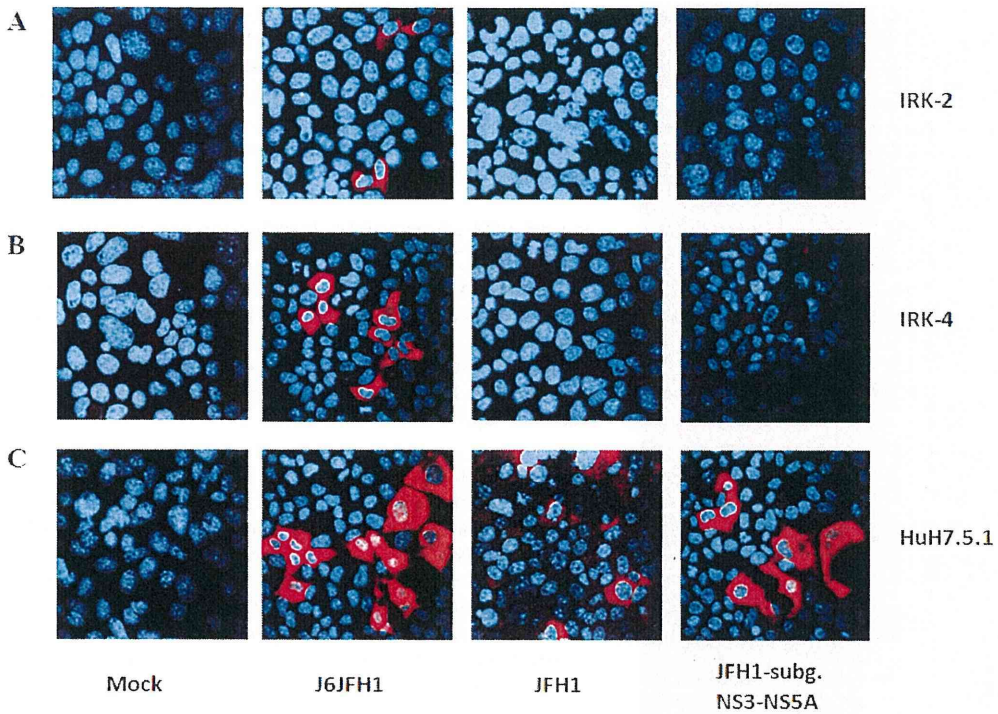

Figure 7. Detection of HCV-NS5A protein in IRK-2 (A), IRK-4 (B) and HuH-7.5 cells (C) by IF 5 days after transfection with J6JFH1, FL-JFH1 or subgenomic JFH1-RNA.
doi:10.1371/journal.pone.0021284.g007

detection was performed on a ZEISS LSM 510 Meta confocal microscope (Zeiss, Jena, Germany).

Detection of cell death

Culture medium was collected from HCV infected and control cells and used for measuring lactate dehydrogenase (LDH) levels using an LDH cytotoxicity detection kit (Takara Biomedicals, Tokyo, Japan). Light absorbance was then measured according to the manufacturer's protocol.

Ethic Statement

This study was carried out in strict accordance with the recommendations in the Guide for the Care and Use of Laboratory Animals of the National Institutes of Health. The protocol was approved by the Committee on the Ethics of Animal Experiments in the Animal Safety Center, Hokkaido University, Japan. All mice were used according to the guidelines of the institutional animal care and use committee of Hokkaido University, who approved this study as ID number: 08-0243, " Analysis of immune modulation by toll-like receptors".

Supporting Information

Figure S1 RT detection of TLR3, TLR7, RIG-I, and IPS-1 expression in mouse hepatocytes. GAPDH expression was used as internal control, and RNA from CD11c+ spleenocytes (dendritic cells) was used as positive control.
(TIF)

Figure S2 Proliferation of HCV in IPS-1, TICAM-1(TRIF) and IFNAR-knockout mouse hepatocytes over time as detected by quantitative real-time RT-PCR analysis of HCV-RNA levels. JFH1GND transfection into IPS-1 knockout cells was used as a negative control to exclude non replicating HCV RNA. The data plotted represent the average +/− STD of 3 different experiments.
(TIF)

Figure S3 RT detection of CD81, Occludin, Claudin 1, SRB1, and LDL receptor expression in primary, IRK4 and IPK17 mouse hepatocytes. GAPDH expression was used as internal control.
(TIF)

Figure S4 Estimation of the transfection efficiency of lentivirus vector expressing green fluorescent protein (GFP) as a reporter, together with hCD81 or hOccludin. 48 hours after transfection with the lentivirus vector, cells were trypsinized and GFP positive cells were detected by BD FACSCalibur (BD Biosciences).
(TIF)

Figure S5 HCV infection of IRK2 cells transfected with lentivirus expressing hCD81 and/or hOccludin. IRK2 cells were transfected with lentivirus expressing empty vector (A), hCD81 (B), hOccludin (C) or hCD81 and hOccludin (D) at a MOI of 10. After 48 hours, the cells were infected with concentrated J6JFH1 transfected 7.5.1 culture medium. After a further three hours, cells were washed with PBS and incubated in fresh medium. After another 48 hours, HCV infection was examined through the detection of HCV-NS5a protein expression by immunofluorescence staining.
(TIF)

Figure S6 HCVpp entry into mouse cells. A similar number of IPK17 and HuH7.5.1 were cultured in triplicate. IPK17 cells were only transfected with lentivirus expressing hCD81, while HuH7.5.1 cells were transfected with empty vector at a MOI of

10. After 48 hours, the medium was replaced with a new medium containing mock VSVG-pp or HCVpp expressing luciferase. After another 48 hours, pseudoparticles entry was determined by measuring the luciferase activity. In order to compare the HCVpp entry between IPK17 and HuH7.5.1 cells, the luciferase expression from VSV-Gpp entry was used an internal control, while that from HCVpp was plotted relatively.
(TIF)

Acknowledgments

We want to thank Dr. Michinori Kohara (Tokyo Metropolitan Institute for Medical Science, Tokyo, Japan); Dr. Tadatsugu Taniguchi (University of Tokyo, Yokyo, Japan); Dr. Thomas Pietschmann (Division of Experimental Virology, TWINCORE, Hannover, Germany); and Dr. Makoto Hijikata (The Institute for Virus Research, Kyoto University, Japan) for their generous supply of research material. Dr. Hussein H. Aly was supported by a JSPS postdoctoral fellowship from the Japan Society for the Promotion of Science.

Author Contributions

Conceived and designed the experiments: HHA TS. Performed the experiments: HHA HO. Analyzed the data: HHA MM HO HS TS. Contributed reagents/materials/analysis tools: KS TW. Wrote the paper: HHA.

References

1. Seto WK, Lai CL, Fung J, Hung I, Yuen J, et al. (2010) Natural history of chronic hepatitis C: Genotype 1 versus genotype 6. J Hepatol.
2. Uprichard SL, Chung J, Chisari FV, Wakita T (2006) Replication of a hepatitis C virus replicon clone in mouse cells. Virol J 3: 89.
3. Ploss A, Evans MJ, Gaysinskaya VA, Panis M, You H, et al. (2009) Human occludin is a hepatitis C virus entry factor required for infection of mouse cells. Nature 457: 882–886.
4. Diamond MS (2009) Mechanisms of evasion of the type I interferon antiviral response by flaviviruses. J Interferon Cytokine Res 29: 521–530.
5. O'Neill LA, Bowie AG (2010) Sensing and signaling in antiviral innate immunity. Curr Biol 20: R328–333.
6. Platanias LC (2005) Mechanisms of type-I- and type-II-interferon-mediated signalling. Nat Rev Immunol 5: 375–386.
7. Tanaka Y, Nishida N, Sugiyama M, Kurosaki M, Matsuura K, et al. (2009) Genome-wide association of IL28B with response to pegylated interferon-alpha and ribavirin therapy for chronic hepatitis C. Nat Genet 41: 1105–1109.
8. Thompson AJ, Muir AJ, Sulkowski MS, Ge D, Fellay J, et al. (2010) Interleukin-28B polymorphism improves viral kinetics and is the strongest pretreatment predictor of sustained virologic response in genotype 1 hepatitis C virus. Gastroenterology 139: 120–129. e118.
9. Sumpter R, Jr., Loo YM, Foy E, Li K, Yoneyama M, et al. (2005) Regulating intracellular antiviral defense and permissiveness to hepatitis C virus RNA replication through a cellular RNA helicase, RIG-I. J Virol 79: 2689–2699.
10. Foy E, Li K, Sumpter R, Jr., Loo YM, Johnson CL, et al. (2005) Control of antiviral defenses through hepatitis C virus disruption of retinoic acid-inducible gene-I signaling. Proc Natl Acad Sci U S A 102: 2986–2991.
11. Oshiumi H, Ikeda M, Matsumoto M, Watanabe A, Takeuchi O, et al. (2010) Hepatitis C virus core protein abrogates the DDX3 function that enhances IPS-1-mediated IFN-beta induction. PLoS One 5: e14258.
12. Oshiumi H, Miyashita M, Inoue N, Okabe M, Matsumoto M, et al. (2010) The ubiquitin ligase Riplet is essential for RIG-I-dependent innate immune responses to RNA virus infection. Cell Host Microbe 8: 496–509.
13. Ishiyama T, Kano J, Minami Y, Iijima T, Morishita Y, et al. (2003) Expression of HNFs and C/EBP alpha is correlated with immunocytochemical differentiation of cell lines derived from human hepatocellular carcinomas, hepatoblastomas and immortalized hepatocytes. Cancer Sci 94: 757–763.
14. Berg CP, Schlosser SF, Neukirchen DK, Papadakis C, Gregor M, et al. (2009) Hepatitis C virus core protein induces apoptosis-like caspase independent cell death. Virol J 6: 213.
15. Deng L, Adachi T, Kitayama K, Bungyoku Y, Kitazawa S, et al. (2008) Hepatitis C virus infection induces apoptosis through a Bax-triggered, mitochondrion-mediated, caspase 3-dependent pathway. J Virol 82: 10375–10385.
16. Zhu H, Dong H, Eksioglu E, Hemming A, Cao M, et al. (2007) Hepatitis C virus triggers apoptosis of a newly developed hepatoma cell line through antiviral defense system. Gastroenterology 133: 1649–1659.
17. Ray RB, Meyer K, Ray R (1996) Suppression of apoptotic cell death by hepatitis C virus core protein. Virology 226: 176–182.
18. Mankouri J, Dallas ML, Hughes ME, Griffin SD, Macdonald A, et al. (2009) Suppression of a pro-apoptotic K+ channel as a mechanism for hepatitis C virus persistence. Proc Natl Acad Sci U S A 106: 15903–15908.
19. Ladu S, Calvisi DF, Conner EA, Farina M, Factor VM, et al. (2008) E2F1 inhibits c-Myc-driven apoptosis via PIK3CA/Akt/mTOR and COX-2 in a mouse model of human liver cancer. Gastroenterology 135: 1322–1332.
20. Lowe SW, Lin AW (2000) Apoptosis in cancer. Carcinogenesis 21: 485–495.
21. Schulze-Bergkamen H, Krammer PH (2004) Apoptosis in cancer--implications for therapy. Semin Oncol 31: 90–119.
22. Ebihara T, Shingai M, Matsumoto M, Wakita T, Seya T (2008) Hepatitis C virus-infected hepatocytes extrinsically modulate dendritic cell maturation to activate T cells and natural killer cells. Hepatology 48: 48–58.
23. Mateu G, Donis RO, Wakita T, Bukh J, Grakoui A (2008) Intragenotypic JFH1 based recombinant hepatitis C virus produces high levels of infectious particles but causes increased cell death. Virology 376: 397–407.
24. Bitzegeio J, Bankwitz D, Hueging K, Haid S, Brohm C, et al. (2010) Adaptation of hepatitis C virus to mouse CD81 permits infection of mouse cells in the absence of human entry factors. PLoS Pathog 6: e1000978.
25. Lin LT, Noyce RS, Pham TN, Wilson JA, Sisson GR, et al. (2010) Replication of subgenomic hepatitis C virus replicons in mouse fibroblasts is facilitated by deletion of interferon regulatory factor 3 and expression of liver-specific microRNA 122. J Virol 84: 9170–9180.
26. Ishigami A, Fujita T, Handa S, Shirasawa T, Koseki H, et al. (2002) Senescence marker protein-30 knockout mouse liver is highly susceptible to tumor necrosis factor-alpha- and Fas-mediated apoptosis. Am J Pathol 161: 1273–1281.
27. Akazawa T, Ebihara T, Okuno M, Okuda Y, Shingai M, et al. (2007) Antitumor NK activation induced by the Toll-like receptor 3-TICAM-1 (TRIF) pathway in myeloid dendritic cells. Proc Natl Acad Sci U S A 104: 252–257.
28. Ebihara T, Azuma M, Oshiumi H, Kasamatsu J, Iwabuchi K, et al. (2010) Identification of a polyI:C-inducible membrane protein that participates in dendritic cell-mediated natural killer cell activation. J Exp Med 207: 2675–2687.
29. Aly HH, Qi Y, Atsuzawa K, Usuda N, Takada Y, et al. (2009) Strain-dependent viral dynamics and virus-cell interactions in a novel in vitro system supporting the life cycle of blood-borne hepatitis C virus. Hepatology 50: 689–696.
30. Aly HH, Shimotohno K, Hijikata M (2009) 3D cultured immortalized human hepatocytes useful to develop drugs for blood-borne HCV. Biochem Biophys Res Commun 379: 330–334.
31. Wakita T, Pietschmann T, Kato T, Date T, Miyamoto M, et al. (2005) Production of infectious hepatitis C virus in tissue culture from a cloned viral genome. Nat Med 11: 791–796.
32. Aly HH, Watashi K, Hijikata M, Kaneko H, Takada Y, et al. (2007) Serum-derived hepatitis C virus infectivity in interferon regulatory factor-7-suppressed human primary hepatocytes. J Hepatol 46: 26–36.
33. Haid S, Windisch MP, Bartenschlager R, Pietschmann T (2010) Mouse-specific residues of claudin-1 limit hepatitis C virus genotype 2a infection in a human hepatocyte cell line. J Virol 84: 964–975.

Cyclosporin A Associated Helicase-Like Protein Facilitates the Association of Hepatitis C Virus RNA Polymerase with Its Cellular Cyclophilin B

Kengo Morohashi[1☯], Hiroeki Sahara[2*], Koichi Watashi[3☯], Kazuki Iwabata[1], Takashi Sunoki[1], Kouji Kuramochi[1], Kaori Takakusagi[1], Hiroki Miyashita[4], Noriyuki Sato[4], Atsushi Tanabe[2], Kunitada Shimotohno[5], Susumu Kobayashi[1], Kengo Sakaguchi[1], Fumio Sugawara[1]

1 Genome and Drug Research Center, Tokyo University of Science, Noda, Chiba, Japan, **2** Laboratory of Biology, Azabu University School of Veterinary Medicine, Sagamihara, Kanagawa, Japan, **3** Department of Virology II, National Institute of Infectious Diseases, Shinjuku-ku, Tokyo, Japan, **4** Department of Pathology, Sapporo Medical University School of Medicine, Sapporo, Hokkaido, Japan, **5** Research Institute, Chiba Institute of Technology, Narashino, Chiba, Japan

Abstract

Background: Cyclosporin A (CsA) is well known as an immunosuppressive drug useful for allogeneic transplantation. It has been reported that CsA inhibits hepatitis C virus (HCV) genome replication, which indicates that cellular targets of CsA regulate the viral replication. However, the regulation mechanisms of HCV replication governed by CsA target proteins have not been fully understood.

Principal Findings: Here we show a chemical biology approach that elucidates a novel mechanism of HCV replication. We developed a phage display screening to investigate compound-peptide interaction and identified a novel cellular target molecule of CsA. This protein, named CsA associated helicase-like protein (CAHL), possessed RNA-dependent ATPase activity that was negated by treatment with CsA. The downregulation of CAHL in the cells resulted in a decrease of HCV genome replication. CAHL formed a complex with HCV-derived RNA polymerase NS5B and host-derived cyclophilin B (CyPB), known as a cellular cofactor for HCV replication, to regulate NS5B-CyPB interaction.

Conclusions: We found a cellular factor, CAHL, as CsA associated helicase-like protein, which would form trimer complex with CyPB and NS5B of HCV. The strategy using a chemical compound and identifying its target molecule by our phage display analysis is useful to reveal a novel mechanism underlying cellular and viral physiology.

Citation: Morohashi K, Sahara H, Watashi K, Iwabata K, Sunoki T, et al. (2011) Cyclosporin A Associated Helicase-Like Protein Facilitates the Association of Hepatitis C Virus RNA Polymerase with Its Cellular Cyclophilin B. PLoS ONE 6(4): e18285. doi:10.1371/journal.pone.0018285

Editor: Robyn Klein, Washington University, United States of America

Received April 15, 2010; **Accepted** March 2, 2011; **Published** April 29, 2011

Funding: This work was supported by The Promotion and Mutual Aid Corporation for Private Schools of Japan, Grant-in-Aid for Matching Fund Subsidy for Private Universities. The funders had no role in study design, data collection and analysis, decision to publish, or preparation of the manuscript.

Competing Interests: The authors have declared that no competing interests exist.

* E-mail: sahara@azabu-u.ac.jp

☯ These authors contributed equally to this work.

Introduction

Cyclosporin A (CsA) possesses immunosuppressive effects and is widely used for allogeneic transplantation [1]. These therapeutic effects of CsA, in particular downregulation of interleukin 2 (IL-2) production by T cells, are considered to be responsible for the suppression of immunological events via cellular immunology [2,3]. Its mechanism is widely believed to include CsA binding to its primary cytoplasmic receptor cyclophilin A (CyPA). This CsA/CyPA complex inhibits the phosphatase activity of calcineurin, which is essential for the activation of nuclear factor of activated T cells (NFAT) transcription factors and their downstream cytokine production [2–5]. The cyclophilins (CyP), identified as cytoplasmic receptors for CsA are a family of peptidylprolyl cis-trans isomerases (PPIase) and include more than ten subtypes [6–8]. Recently, it was reported that several CyPs regulated hepatitis C virus (HCV) replication; CyPA binds to HCV NS5A and NS5B proteins. CyPB also interacted with HCV NS5A and NS5B [9–11]. The interaction of CyPB stimulates the RNA binding activity of NS5B. These viral-cellular interaction mechanisms were revealed by a chemical biological analysis focusing on an anti-viral characteristic of CsA. However, it has not been fully understood how a series of CsA-target proteins regulate HCV replication. We obtained the data suggesting the possibility that CsA target factor(s) other than CyP family also modify HCV replication.

To exploit a novel drug target is a challenging but a powerful strategy to elucidate unknown aspects of cellular physiology that are modified by the compound. In this study, we identify a CsA binding factor by a phage display method. There are various methods to isolate targets of small molecules. Most of the methods, however, require tagged small molecules for screening to separate the drug and protein complex. The steps to synthesize tagged small molecules are technically limited in the case of complicated molecules such as CsA. To overcome this limitation, we recently developed a labeling method that can be theoretically utilized for

any chemical substance [12]. A highly reactive carbene induced by UV irradiation reacts with CsA, resulting in the production of immobilized CsA in a nonspecific manner. By using the photoaffinity method, we successfully immobilized CsA on resins and performed phage display screening. This method cloned a CsA associated helicase-like protein, which we termed CAHL, and this protein was shown to interact with HCV replication machinery. Our result presents an example for the chemical biological method that could facilitate to reveal a mechanism of viral-cellular interaction.

Results

Phage display screening with immobilized CsA isolated CsA associated helicase-like protein, CAHL

To explore CsA binding proteins, we applied a chemical biology approach. In general, small molecule is necessary to be chemically modified such as biotinylated to be immobilized on solid surface for isolation of binding proteins. However, due to the structural complexity of CsA, it is technically challenging to chemically modify a certain residue of CsA. Therefore, we took advantage of photoaffinity coupling method, which we previously developed [12]. The highly reactive carbene induced by UV irradiation reacted with CsA, resulting in the production of immobilized CsA on solid surface in a nonspecific manner (Fig. 1A). We performed phage display screening with multiple cycles that consist of binding, washing, recovery and amplification (Fig. 1B). We used phage particles randomly displayed 12 amino acids as a library [13]. Through the screening cycles, the ratios of eluted phage particles associated with CsA-immobilized resins comparing to input were dramatically increased (Fig. 1C). We randomly picked up 22 single phage clones from the sixth panning elution (Table S1). Five out of the 22 phage clones were identical, and we called it phage #13. In order to validate the binding specificity of the phage, we amplified phage #13 and measure the ratio of eluted phage titer with CsA and mock resins, which were treated with MeOH to block photoaffinity reaction. The ratio of the phage #13 was 3.75, whereas randomly picked up phage was 1.00. These results indicated that the phage #13 specifically associated with CsA-immobilized resins.

CAHL has an RNA-dependent ATP hydrolysis activity

Phage #13 was predicted to display amino acids, LVFGTLLGQLRA, in the carboxyl terminus of its phage-coat protein, which is responsible for interaction with CsA. We searched the protein database to find proteins that showed similarities to the LVFGTLLGQLRA sequence. As a result of the search, we found a protein with a sequence identical to LLGQLRA, encoded by a gene accession number NM_022828 in the NCBI database. NM_022828 is predicted to encodes 1430 amino acid protein that has a couple of conserved domains, such as DEXHc helicase, RNA-dependent ATPase and ankyrin repeat (Fig. 2A; Fig S1). LLGQLRA sequence is located in the middle region of the protein (amino acids 940–946), where is no known conserved motif is found (Fig. 2A). Since it has not been reported on its biological functions, hereafter we refer to the NM_022828 as CsA-associated helicase-like protein, CAHL. To confirm the interaction between CAHL and CsA, we prepared a recombinant C-terminal protein of CAHL (named CAHL-C) that consisted of amino acids 761 to 1430 (Fig. 2B) including LLGQLRA motif, and performed surface plasmon resonance (SPR) analysis. It was difficult to use a full-length CAHL for *in vitro* pull-down assays since obtaining enough amount of full-length CAHL for SPR was technically challenging due to high insolubility. Considering that CsA binding sequence

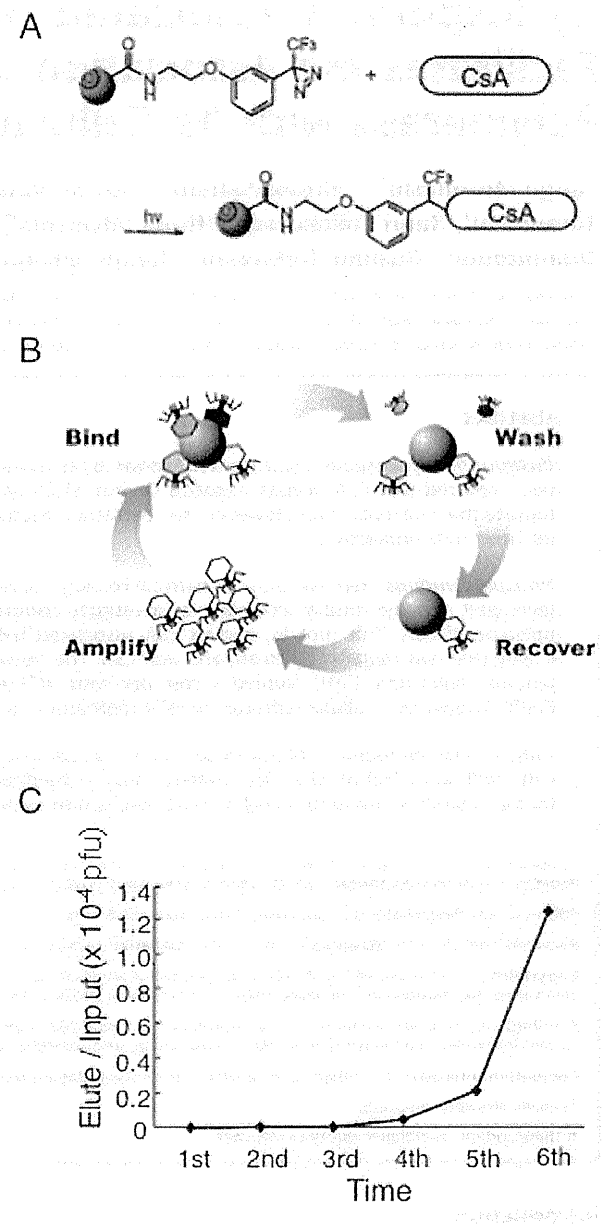

Figure 1. Immobilization of CsA and phage display screening. (A) A schematic diagram of CsA immobilization on photoaffinity resins. (B) Procedure of phage display screening. (C) Relative enrichment of phage particles. Relative enrichment was determined by the relationship between phage titer of elution from a CsA immobilized resins and input.
doi:10.1371/journal.pone.0018285.g001

found by the phage display screening is located C-terminus of CAHL, we used CAHL-C protein. A specific binding response with CsA was observed ($KD = 1.2 \times 10^{-7}$ M), whereas those with FK506, which is an immunosuppressant and has no HCV-inhibitory activity, were significantly weak ($KD = 2.5 \times 10^{-6}$ M) (Fig. 2C). Since CAHL was predicted to be RNA-dependent ATPase based on conserved domains (Fig. 2A), we measured the ATPase activity of CAHL in the presence and absence of RNA. As shown in Fig.2D, RNA-dependent ATP hydrolytic activity of CAHL-C was clearly observed, and this activity was suppressed in

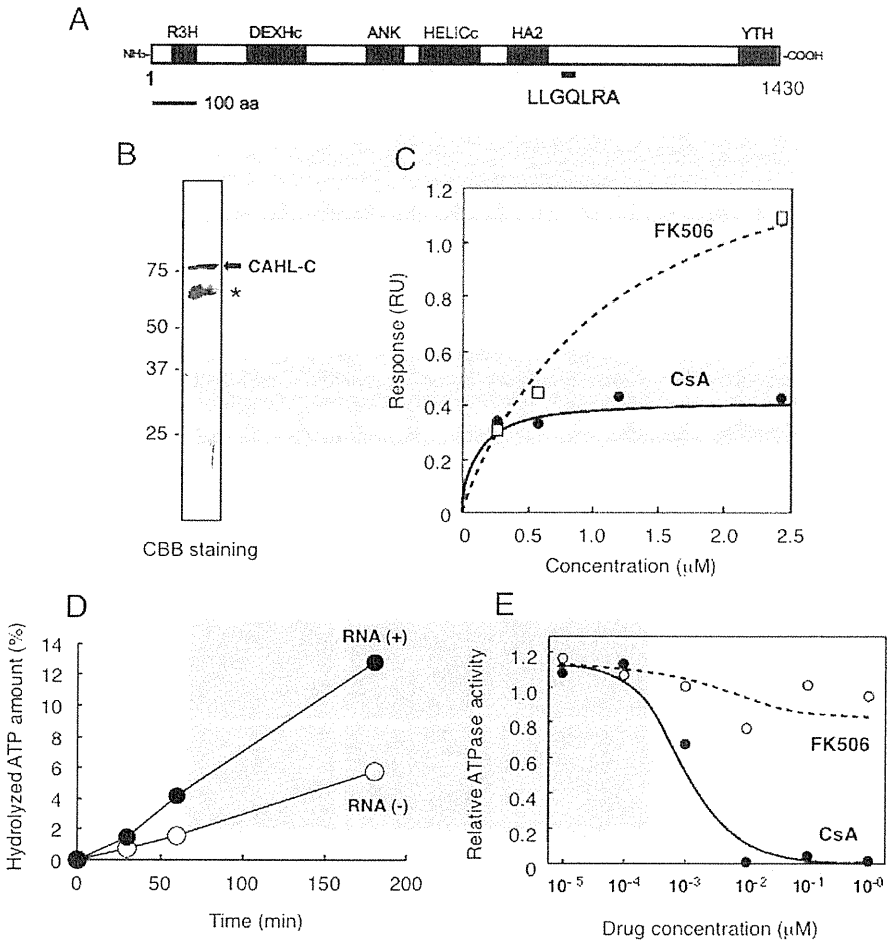

Figure 2. Cloning of CsA associated helicase-like protein (CAHL) by phage display screening. (A) Schematic representation of CAHL protein. R3H (*cd*02325), DEXHc (*cd*00269), ANK (*cd*00204), HELICc (*smart*00490), HA2 (*pfam*04408) and YTH (*pfam*04146) motifs were found by a CD search (http://www.ncbi.nlm.nih.gov/Structure/edd/wrpsb.cgi). Underline indicates a region of the LLGQRA amino acid sequence identical to the CsA-associated sequence displayed on phage #13. (B) Purified recombinant CAHL-C protein was confirmed by SDS-PAGE analysis (arrow). Asterisk indicates degraded products. (C) A kinetic plot and binding isotherm for binding of CsA (closed circle) and FK506 (opened square) to CAHL-C sensor chips in concentrations ranging from 0.25 to 2.5 mM. The estimated KD value of interaction between CAHL-C and CsA or FK506 was 1.2×10^{-7} or 2.5×10^{-6} M, respectively. (D) RNA-dependent ATP hydrolytic activities of CAHL. Filled and open circles indicate ATP hydrolytic activities of CAHL in the presence (closed circle) or absence (opened circle) of total RNA extracted from liver cells, respectively. (E) CsA inhibitory effects on ATP hydrolytic activities of CAHL. Filled and open circles indicate ATP hydrolytic activities with CsA (closed circle) or FK506 (opened circle), respectively.
doi:10.1371/journal.pone.0018285.g002

a dose-dependent manner when CsA, but not FK506 (Fig. 2E). A difference of inhibitory effects of CsA and FK506 on CAHL-C hydrolytic activity is more than 2-orders of magnitude. Considering that the difference of *KD*s of CsA and FK506 values measured by SPR, CsA association with CAHL would significantly affect on the activity. These results indicate that CAHL had RNA-dependent ATPase activity and was specifically inhibited by CsA.

CAHL is localized in ER and its expression is up-regulated by TNF-α treatment

Since biological functions of CAHL were unknown, we investigated the biological background of the CAHL gene. We first performed RNA blotting analysis and RT-PCR using normal human tissues and tumor cells. As shown in Fig. 3A, CAHL-transcripts with approximately 1.6 kbp were detected in both human hepatoma Huh-7 cells and MH-14 cells, which do not and do carry the HCV subgenome replicon, respectively, whereas much less was detected in normal liver tissues. RT-PCR analysis revealed that in other normal tissues (though not testis) little or no expression of CAHL was observed as compared the house-keeping gene G6PDH, whereas clear expression of it was detected in all the tumor cell lines examined (Fig. 3B). Since the CAHL expression was very little in the normal liver tissues, a question was arisen: how is CAHL expression regulated? It is possible that CAHL could be induced by inflammation caused by virus infections. To test the hypothesis, we observed whether CAHL expressions are induced by inflammatory signals. Indeed, CAHL in normal liver cells was upregulated in the presence of a proinflammatory cytokine, tumor necrosis factor (TNF)-α with dose dependent manner (Fig. 3C), suggesting that CAHL can express to some extent in the liver under chronic hepatitis. Next, we observed CAHL subcellular localization in Huh-7 and MH-14 cells using an anti-CAHL antibody (Fig. 3D). Fluorescence derived from CAHL

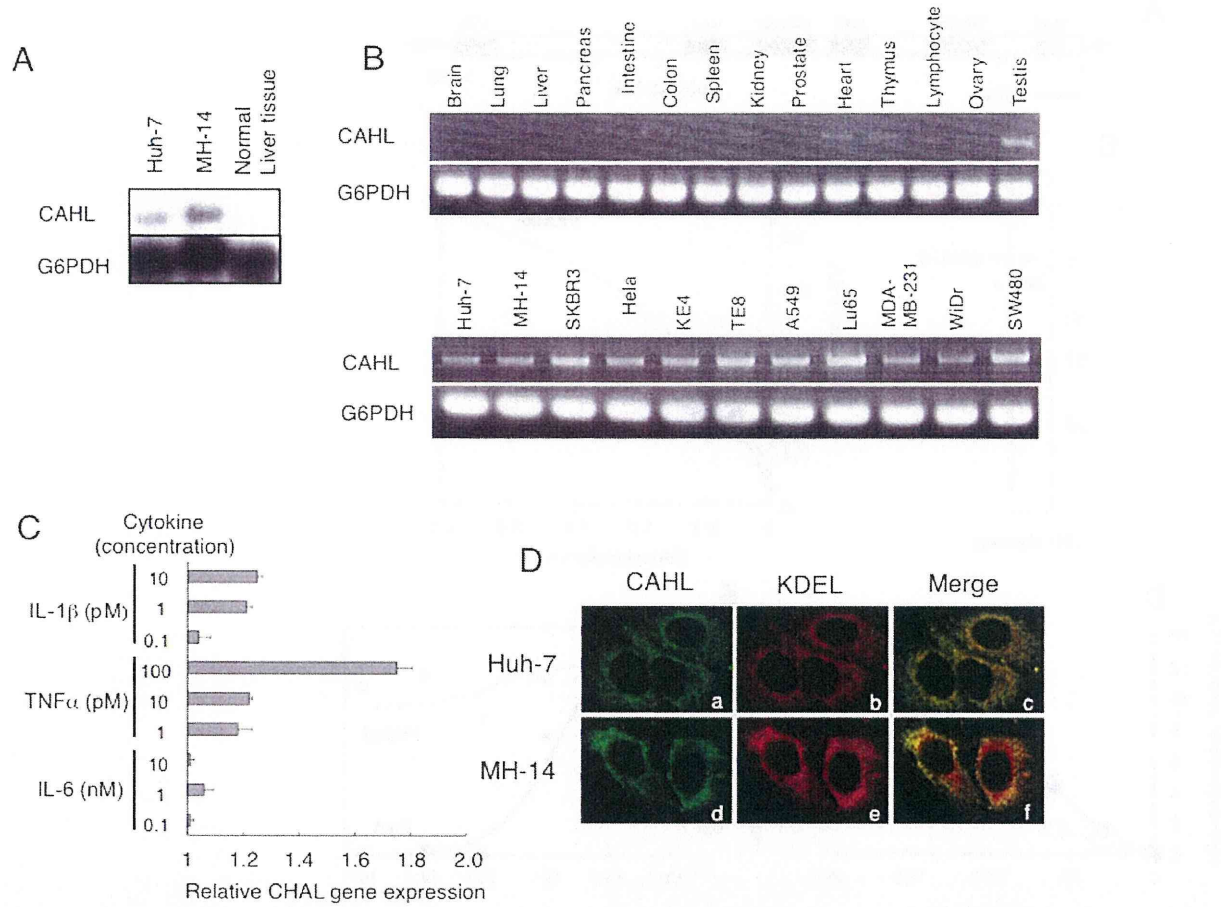

Figure 3. Expression profile of CAHL. (A) For Northern blot analysis, CAHL and G6PDH as an internal control were detected in RNAs derived from Huh-7 and MH-14 cells, as well as normal liver tissues. (B) RT-PCR analysis for CAHL, and G6PDH as an internal control, were performed using RNAs derived from normal human tissues and tumor cells. (C) CAHL in normal liver cells was upregulated by TNF-α. Normal liver cells were cultured in the presence of proinflammatory cytokines, IL-1β, TNF-α, and IL-6 at the indicated concentrations for 8 h. Subsequently, cells were harvested, and measurement of these cells derived-CAHL gene expression by quantitative analysis by was performed using the LightCycler system. These data represent as relative rates (1 = non-treated cells). Error bars represent the standard error of the mean. (D) Colocalization of CAHL with KDEL as an endoplasmic reticulum (ER) marker. Indirect immunofluorescence analysis was performed on Huh-7 and MH-14 cells. Cells stained with anti-CAHL (panels a and d, green) and an anti-KDEL mAb (panels b and e, red) for ER identification as a marker used as a primary antibody followed by Alexa Fluor 488-conjugated goat anti-rabbit and 594-conjugated goat anti-mouse antibodies, respectively. Merged images of green and red signals are shown in panels c and f.The optically merged image is representative of most cells examined by laser confocal microscopy. Original magnification: x1000.

doi:10.1371/journal.pone.0018285.g003

demonstrated that CAHL was co-localized with KDEL protein as a marker for endoplasmic reticulum (ER) in both the presence (MH-14 cells) and absence (Huh-7 cells) of the HCV subgenome, indicating that CAHL could localize in ER with HCV independent manner. Moreover, it was observed that CAHL also colocalized with HCV-derived proteins such as NS3, NS4A, NS4B, NS5A and NS5B localized in ER (Fig. S2). Thus, these data strongly suggested that CAHL would localize in ER.

Association of CAHL, NS5B and CyPB

Since CAHL interacts CsA, which has inhibitory effects to HCV replication, it is interesting to investigate the molecular interactions of CAHL and HCV-derived molecules involving the replication machinery. Intriguingly, the purified full-length CAHL fused to GST was coprecipitated with NS5B but not NS3, NS4B or NS5A protein, as shown in Fig. 4A. To determine a regions of NS5B responsible for binding with CAHL, various dissected NS5B proteins were subjected to pull-down assays, resulting in that two separated regions (1–200 aa or 401–520 aa) of NS5B were sufficient for the interaction with CAHL (Fig. 4B). In addition to the CAHL and NS5B interaction, we found interaction between CAHL and CyPB, but not CyPA (Fig. 4C). The interaction of CAHL and CyPB was disrupted with presence of CsA, whereas the association of CAHL with NS5B was not (Fig. 4D). These results suggest that trimer complex consisting of CAHL, CyPB and NS5B could form.

CAHL has a main role in HCV-replication via NS5B

The finding that CAHL structurally associated with the CyPB/NS5B complex in cell-free assessment prompted us to examine whether this trimer complex could act for HCV genome replication *in vivo*. First, five small interference RNAs (siRNA)

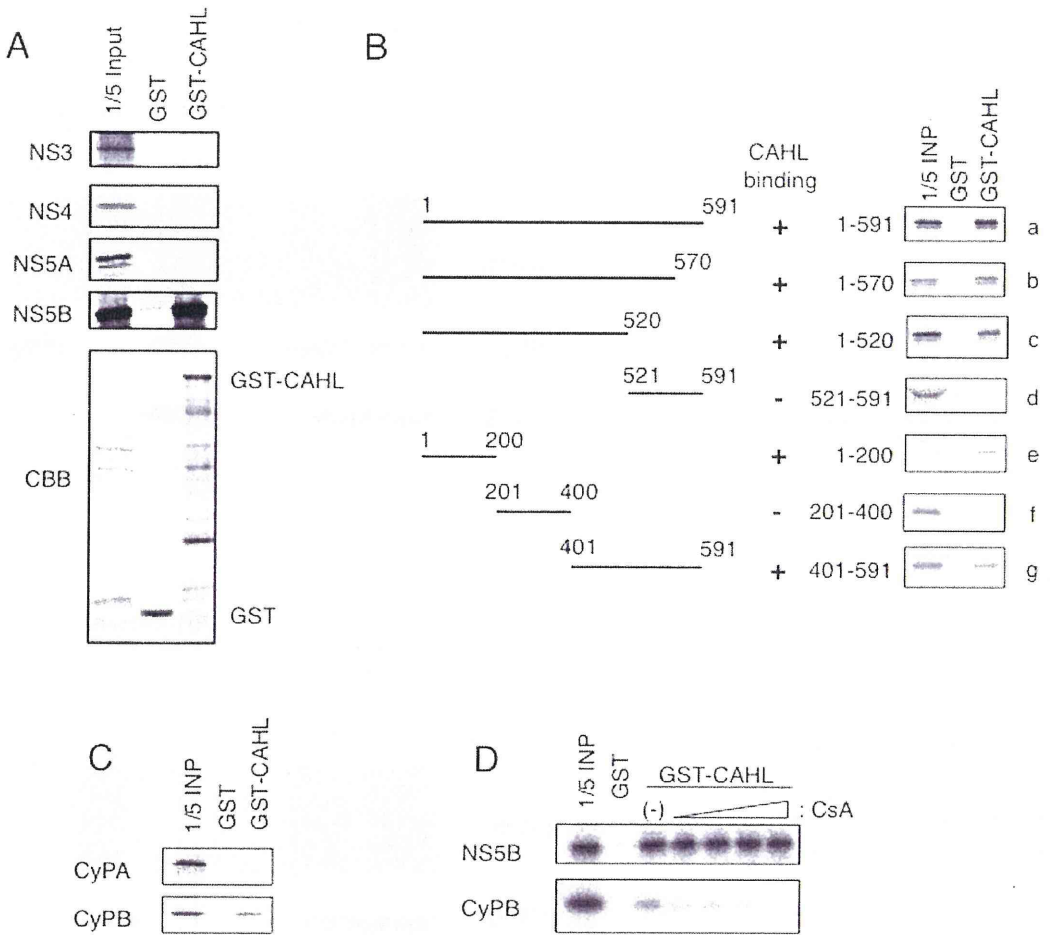

Figure 4. CAHL interacted with HCV NS5B and CyPB. (A) [^{35}S]-labeled in vitro translation products of HCV NS3, NS4B, NS5A, and NS5B were incubated with a recombinant GST fusion protein of CAHL (GST-CAHL) or GST as a negative control. "1/5 input" designates the signal for 1/5 the amount of the [^{35}S]-labeled product used in the pull-down assay. CBB staining patterns for the pulled-down proteins are shown in the bottom panel. (B) Mapping of the regions of NS5B responsible for the interaction with CAHL. At the left of the panel, schematic representations of the full-length and truncated mutants of NS5B are shown. The numbers indicate the amino acid residue numbers in NS5B. "CAHL binding" summarizes the results of the GST pull-down assay by +/−. GST pull-down data are presented as described in (A). (C) GST pull-down assay between GST-CAHL and in vitro translated CyPA or CyPB was performed as described in (A). (D) The interaction of CAHL with CyPB was disrupted by CsA treatment. GST pull-down assay between GST-CAHL and NS5B was performed in the absence and presence of CsA. The concentrations of CsA in lanes 4–7 are 1, 2, 8, and 20 μg/ml, respectively.
doi:10.1371/journal.pone.0018285.g004

specific for the CAHL gene (si-1, -2, -3, -4, and -5) were individually transfected into MH-14 cells to examine RNA sequence induced effectively down-regulation. When si-3 siRNA was transfected into cells, the endogenous CAHL gene expression reduced approximately 90% compared with si-control (treatment with siRNA for non-target gene) (Fig. S3), and among them, si-3 induced down-regulation of CAHL gene expression most effectively. Subsequently, we applied short hairpin RNA (shRNA) technology to stably knockdown CAHL gene expression in MH14 cells. We cloned DNA oligo coding the effective siRNA against CAHL gene into pLKO.1-puro shRNA vector. Lentivirus packed with shRNA against CAHL (sh-CAHL) or non-targeting shRNA (sh-control) were introduced into MH14 cells, and then these cells were cultured in the presence puromycin. As a result, we successfully obtained stably CAHL gene knockdown cell line, which reduced approximately to 6-fold compared with sh-control (Fig. 5A). In these sh-CAHL cells, HCV RNA was decreased approximately to 4-fold less than that in the sh-control cells (Fig. 5B). Furthermore, ectopic expression of CAHL increased the HCV replication level in a dose-dependent manner (Fig. 5C). These results suggest that CAHL positively plays in HCV replication.

To investigate the outcome of the interaction of CAHL with NS5B/CyPB, we performed RNA binding activity assay using sh-CAHL cells. NS5B is a viral RNA-dependent RNA polymerase and possesses RNA binding activity [11]. Indeed, NS5B formed a complex on RNA-immobilized sepharose together with CyPB and CAHL (lane 4 in Fig. 6A). However, shRNA-mediated depletion of endogenous CAHL dissociated CyPB from the NS5B/RNA complex (lane 6 in Fig. 6A), indicating that CAHL mediates the association of CyPB with NS5B/RNA. Moreover, when CsA was added to sh-CAHL cells, both CAHL and CyPB were dissociated from RNA (lane 6 in Fig. 6B). Thus, the possibility is suggested that the promotion of CyPB-NS5B complex association by CAHL is related with the stimulatory role of CAHL in HCV replication.

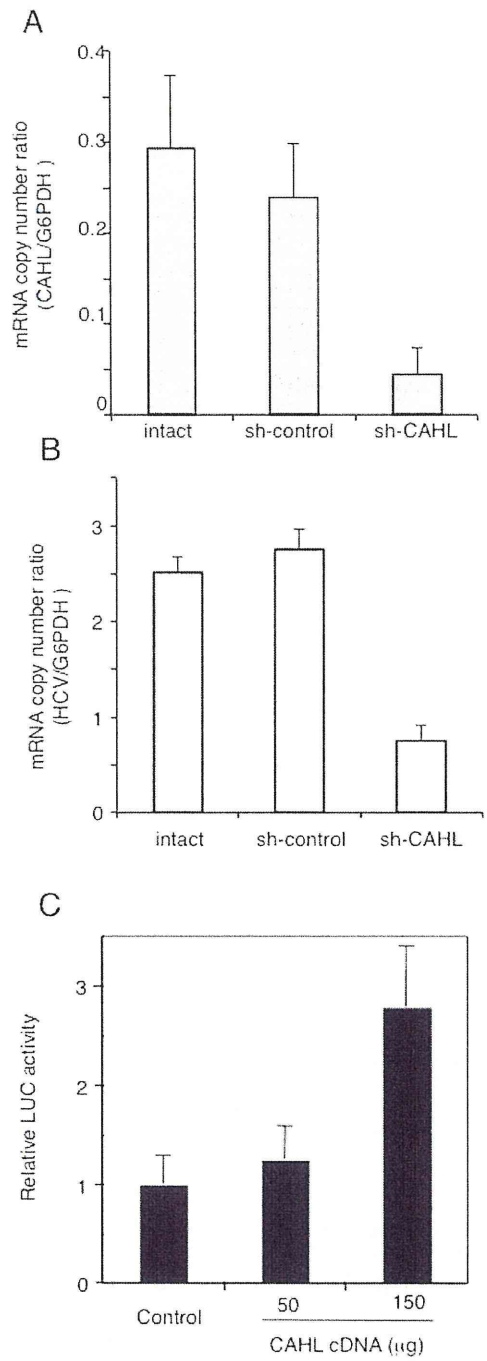

Figure 5. Establishment stably CAHL knockdown cell. (A) Lentivirus packed with shRNA against CAHL (sh-CAHL) or non-targeting shRNA (sh-control) were introduced into MH14 cells. Total RNAs were harvested and the absolute mRNA copy numbers of CAHL were examined by quantitative real time RT-PCR. (B) The same samples of total RNAs were used for the measurement of the absolute RNA copy number of the HCV genome by quantitative real time RT-PCR. (C) Cured MH-14 cells were transfected with LMH14 RNA reporter together with the expression plasmid for CAHL or the corresponding empty vector. At four days post-transfection, luciferase activities were measured. These results (A–C) represent the means of three independent experiments.
doi:10.1371/journal.pone.0018285.g005

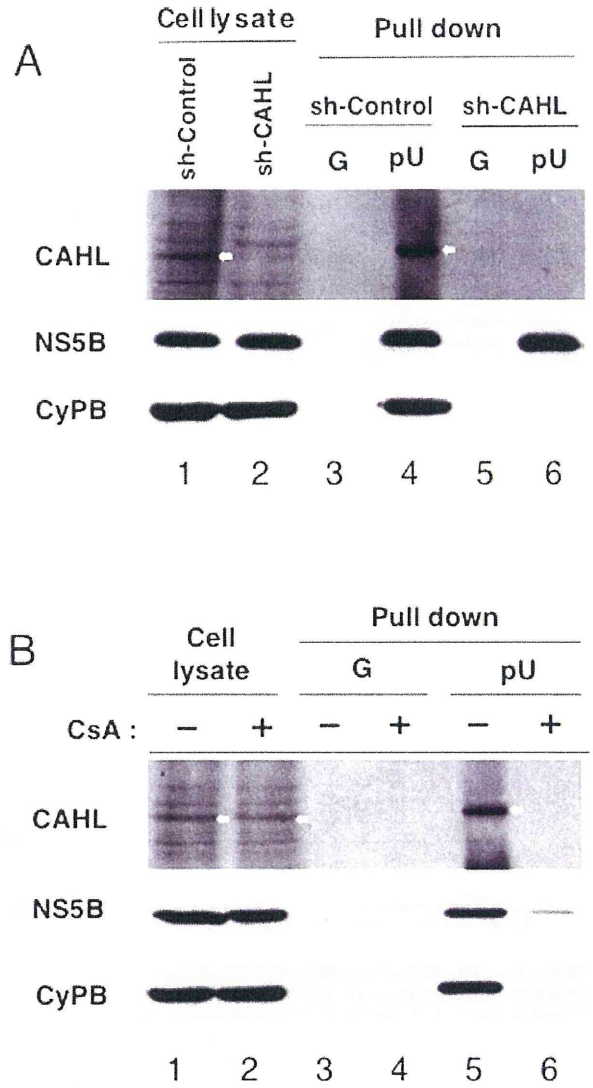

Figure 6. CAHL associated with the CyPB/NS5B complex plays critical roles in HCV replication. (A) Cells (sh-control or sh-CAHL cells) were harvested and analyzed protein expressions by using anti-CAHL, anti-NS5B, and anti-CyPB antibodies. White arrows indicate CAHL protein. (B) Cells were treated with or without 2 μg/ml CsA for 24 h, and then harvested and analyzed. These results were reproduced in three independent experiments. White arrows indicate CAHL protein.
doi:10.1371/journal.pone.0018285.g006

Discussion

Phage display, invented by Smith and Petrenko, is a versatile method for the detection of small molecule-binding proteins [14]. The technique can also be used to identify binding sites within the target protein itself. The combination of screening a library of phage-displayed peptides and analysis of affinity-selected peptides is anticipated to become a powerful tool for identifying drug-binding sites [15–19]. Screening phage display libraries generally entails immobilizing the drug onto a solid surface [20]. In the conventional method of phage display, small molecules should be converted into biotinylated derivatives and immobilized on a streptavidin-coated matrix. Conventional immobilization requires

the presence of desirable functional groups within the drug molecule as well as a multistep process to prepare the biotinylated derivatives. In contrast to biotinylation, photoimmobilization makes it possible to covalently immobilize drugs on a solid surface without the need for derivatization. We and Kanoh *et al.* have reported the affinity purification of proteins using affinity matrices, in which small molecules are photoimmobilized by photoreaction [12,21]. Because the photoreaction proceeds in a functional group-independent manner, the molecules are immobilized onto the solid surface in a nonoriented fashion. Thus, photoimmobilization can be a useful tool for the comprehensive analysis of drug-binding proteins.

Using this method, we identified CAHL as a novel target protein for CsA. CsA is a natural compound showing multiple biological activities, including an immunosuppressive function, anti-chaperone activity, inhibition of transporter activity and anti-viral activity against human immunodeficiency virus and HCV. Thus far, p-glycoprotein and formyl peptide receptor, as well as CyPs, were reported as binding proteins for CsA [22], which enabled elucidation of the mechanism of the CsA-induced immunosuppressive function, anti-chaperone activity and anti-transporter activity, respectively. Although CyPA promotes HCV replication [11,23,24], we cannot fully explain the whole mode of action of CsA against HCV. CyPB is also reported to regulate HCV replication. It was reported that the HCV replicon showing resistance against the CsA-mediated anti-HCV effect possessed mutations in the coding region for NS5A and NS5B [25,26], indicating that NS5B was one of the determinants for the sensitivity to CsA. However, some such mutations within the NS5B coding region were dropped outside the region interacting with CyPA and CyPB [11,24], leading to the possibility that another cellular protein which is targeted by CsA, binds to NS5B and regulates HCV replication. The CAHL-NS5B regulation machinery is consistent with this idea. Deletion analysis for NS5B demonstrated that two separate regions (1-200aa and 401-520aa) of NS5B are likely to be involved in the interaction with CAHL. These regions are different from the NS5B domain interacting with CyPB (521-591aa) [11], suggesting that NS5B would interact with both CyPB and CAHL at the same time. Indeed, the mutations that induced resistant to CsA, the I432V in NS5B reside inside the regions interacting with CAHL (1-200 aa and 401-520 aa) [26], supported the relevance of CAHL in HCV genome replication. As another aspect, it is interesting that two CsA target molecules interact with each other and NS5B. Although we do not know in detail the implication of the interaction of these two CsA target molecules, CyPB and CAHL, there is a similar example already known: two FK506-binding proteins, P-glycoprotein (P-gp) and FKBP42, associate with each other [27]. In this situation, FKBP42 modulates P-gp function. We do not know in detail how these two target molecules of CsA, CyPB and CAHL both regulate NS5B function, which is a future subject of the study. Currently, a CsA derivative shows remarkable anti-HCV effect in chronic HCV-infected patients in the phase II clinical trial, and its mode of action needs to be fully clarified [28]. Our data suggest a new link of CAHL, in addition to CyP family, with CsA derivative's anti-HCV activity.

Cellular RNA helicases have been reported to be involved in HCV genome replication. DDX3 and DDX6 activate HCV genome replication through yet unknown mechanism [29,30]. RNA helicase p68 (DDX5) interacts with NS5B and supports HCV genome replication in a transient transfection assay [31]. Although the mechanism through which each RNA helicase regulates HCV genome replication may be different, the requirement of cellular RNA helicases for HCV genome replication is interesting for understanding HCV-cellular factors interaction.

CAHL expression in normal liver cells was much less than that in HCV infectious cells such as Huh-7 and MH-14. This is enigmatic since it is not clear how HCV replication start without CAHL, which positively plays HCV replication, at very beginning of HCV infection in normal liver cells. It was reported that a proinflammatory cytokine, TNF-α gene expression in hepatocytes and mononuclear cells derived from HCV carrier increased compared with healthy control [32]. As we here demonstrated CAHL induced by TNF-α, CAHL can express to some extent in the liver under chronic hepatitis C. We also show the association of CAHL with HCV replication. Taken together, CAHL may form a positive feedback loop for HCV replication: CAHL gene expression is induced by TNF-α that is highly upregulated by HCV infection, and CAHL in turn promotes HCV replication. Despite the low expression of CAHL in normal tissues, CAHL may have strong potential as a pharmaceutical target protein. In addition to CsA, isolation of specific inhibitors to the interaction of CAHL and NS5B could allow us to provide effective drug for HCV treatment.

In conclusion, we took advantage of strategy of chemical biology to isolate a cellular factor, CAHL, as CsA associated helicase-like protein, which would form trimer complex with CyPB and NS5B of HCV. These findings not only shed a light on new HCV treatment but also brought about great values of chemical biology to elucidate biological mechanisms of small-molecule and protein interactions.

Materials and Methods

Preparation of CsA-immobilized resins

CsA was purchased from Wako Pure Chemical Industries, Ltd. (Osaka, Japan). CsA-immobilized resins were prepared on photoaffinity resins as described previously [12]. Photoaffinity resins treated with UV irradiation in the absence of CsA were used for negative control.

Phage display screening

10 mg of CsA-immobilized resin was incubated in 1 ml of TBS (50 μM Tris-HCl [pH 8.0] and 150 mM NaCl) for 12 hours or longer before use. Phage screening conditions were performed as previously described [20]. For each panning step, 50 μl of CsA-immobilized resin slurry was added to 1 ml of the T7 phage ($>10^{11}$ pfu) followed by incubation for 8 hours at 4°C. After incubation, the bead slurry was washed 10 times by adding 1 ml of TBST (50 mM Tris-HCl [pH = 8.0], 150 mM NaCl, 0.1% Tween 20). To elute phage particles associated with resins, 100 μl of *Escherichia coli* ($OD_{600} = 0.6$) was added, and incubated for 10 min at 37°C. The phage infected *E. coli* were transferred into 1 ml of *E. coli* ($OD_{600} = 0.6$) and grown until lysed for three hours at 37°C with shaking. For titer check, 10 μl of infected *E. coli* was used.

RNA preparation and plasmid construction

To isolate the CAHL gene, we used total RNA derived from human liver. DNA cloning of the CAHL gene was carried out using a SMART-cDNA isolation kit following the manufacturer's instructions (Clontech Laboratories, CA, USA). In some cases, CAHL cDNA was reconstructed with pcDNA 3.1 myc-HisA (Invitrogen Corp., CA, USA) for overexpression experiments.

Surface plasmon resonance assay

SPR analysis was performed on a BIAcore 3000 (Biacore AB, Uppsala, Sweden). The bacterially expressed CAHL-C was

immobilized covalently on a hydrophilic carboxymethylated dextran matrix on a CM5 sensor chip (Biacore AB) using a standard amine coupling reaction in 10 mM CH_3COONa [pH = 4.0]. Binding analyses were carried out in HBS-EP buffer (10 mM HEPES [pH = 7.4], 150 mM NaCl, 3.4 mM EDTA, 0.005% surfactant P20) containing 8% DMSO at a flow rate of 20 µl/min. Appropriate concentrations of CsA were injected over the flow cell. CyPA or CyPB was not used as a positive control because of two reasons: 1) those CyPs can be used for a positive control as CsA-CyP binding, but not for CsA-CAHL binding, and 2) FK506 doesn't bind CyPs, so that it is difficult to compare association behaviors between FK506 and CsA. The bulk effects of DMSO were subtracted using reference surfaces. To derive binding constants, data were analyzed by means of global fitting using BIAevaluation version 3.1 (Biacore AB).

Preparation of recombinant protein

CAHL-C cDNA encoding C-terminal 761 to1430 amino acids was constructed into pET21a prokaryotic expression vector (Merck, Darmstadt, Germany), which has a His-tag. pET21-CAHL-C construct was transformed into *E.coli* BL21(DE3) strain. After overnight induction with 0.1 mM IPTG at 20°C, recombinant CAHL-C was purified by nickel column chromatography with HisTrap (Amersham biosciences, Uppsala, Sweden) according to a manufacturer's procedure. To concentrate and exchange the buffer, purified CAHL-C was concentrated up to 40 times with PBS by using Amicon Ultra 30 (Millipore, EMD, Germany).

ATPase assay

ATPase activity was measured as described by Okanami *et al.* [33]. Briefly, CAHL-C protein (500 ng) was incubated in 50 µl of helicase/ATPase buffer containing 1 µl of [γ-^{32}P]ATP (1 Ci/µmol) in the presence or absence of 100 ng of total RNA derived from liver at 30°C for 30, 60, and 180 min. An aliquot (10 µl) was removed at the appropriate time and added to 200 ml of a solution containing 50 mM HCl, 5 mM H_3PO_4 and 7% activated charcoal. After the charcoal was precipitated by centrifugation to remove unreacted ATP, 10 µl of the supernatant was subjected to Cerencov counting to quantitate released [^{32}P]phosphate.

Northern blot analysis and reverse transcription PCR (RT-PCR) analysis

Tumor cell-derived total RNA was prepared using an RNeasy Mini Kit (QIAGEN Inc., Hilden, Germany) according to the manufacturer's instructions and then reverse-transcribed to cDNA with Transcriptor First Strand cDNA Synthesis Kit (Roche Applied Science, Mnnheim, Germany). A reverse-transcribed single strand DNA library of normal tissues was purchased from Clontec, Inc. (CA, USA). In Northern blot analysis, RNA samples were loaded to formaldehyde agarose gels and transferred onto a Hybond N membrane (GE Healthcare UK Ltd., Buckinghamshire, England). After UV-crosslinking, the membrane was hybridized with ^{32}P-labeled (Rediprime II, GE Healthcare) gene-specific probe, regions of $CAHL_{2913-4431}$ and human $G6PDH_{454-2016}$ and exposed to film for autoradiography. Measurement of CAHL gene expression by polymerase chain reaction (PCR) was performed using GoTaq Flexi DNA Polymerase (Promega, Co. WI, U.S.A.) and primer sets: forward primer, 5′-GACGGGAAAGGATTGGTCAA-3′ and reverse primer, 5′-CATCACTTCGTGCTTTTT-3′ for detection of CAHL, and forward primer, 5′-GACGAAGCGCAGACAGCGTCATGGCA-3′ and reverse primer, 5′-GCTTGTGGGGGTTCACCCACTTG-3′ for detection of G6PDH.

Quantitative real-time RT-PCR analysis

Total RNAs reverse-transcribed to cDNA were prepared as described above. Measurement of gene expression by quantitative analysis was performed using the LightCycler system (Roche Applied Science). Primers and hybridization probes were synthesized by Nihon Gene Research Laboratory Inc. (Sendai, Japan). Quantitative real time RT-PCR analyses of human glucose-6-phosphate dehydrogenase (G6PDH) and cyclosporin A associated helicase-like protein (CAHL, NM_022828) gene expression were performed using the LightCycler® FastStart DNA MasterPLUS SYBR Green I system (Roche Applied Science) with the following primer sets: forward primer, 5′-CTGCGTTATCCTCACCTTC-3′ and reverse primer, 5′-CGGACGTCATCTGAGTTG-3′ for detection of human G6PDH; forward primer, 5′-GTGT-CTGGACCCCATCCTTA-3′and reverse primer, 5′-CCCAT-CACTTCGTGCTTTTT-3′for detection of CAHL. Gene expression analysis of the HCV genome was performed using the LightCycler® FastStart DNA Master HybProbe system (Roche Applied Science) with the following primer set and probe: forward primer, 5′-CGGGAGAGCCATAGTGG-3′ and reverse primer, 5′-AGTACCACAAGGCCTTTCG-3′, and the fluorogenic probe, 5′-CTGCGGAACCGGTGAGTACAC-3′. PCR amplification of the housekeeping gene, G6PDH, was performed for each sample as control for sample loading and to allow normalization among samples. To determine the absolute copy number of the target transcripts, the fragments of G6PDH or target genes amplified by PCR using the above described primer set were constructed with pCR4®-TOPO® cloning vector (Invitrogen). The concentrations of these purified plasmids were measured by absorbance at 260 nm and copy numbers were calculated from concentration of samples. A standard curve was created by plotting the threshold cycle (Ct) versus the known copy number for each plasmid template in the dilutions. The copy numbers for all unknown samples were determined according to the standard curve using LightCycler version 3.5.3 (Roche Applied Science). To correct for differences in both RNA quality and quantity between samples, each target gene was first normalized by dividing the copy number of the target by the copy number of G6PDH, so that the mRNA copy number of the target was the copy number per the copy number of G6PDH. The initial value was also corrected for the amount of G6PDH indicated as 100% to evaluate the sequential alteration of the mRNA expression level.

Cell culture and transfection of siRNA and cDNA

The human tumor cell lines of breast adenocarcinoma MDA-MB-231, lung adenocarcinoma A-549, colon adenocarcinoma WiDr, hepatocellular carcinoma Huh-7, breast cancer SKBR3, cervical carcinoma HeLa, esophagus cancer KE-4, colon adenocarcinoma SW480, lung cancer Lu65, and esophagus squamous cell carcinoma TE-8 were obtained from Health Science Research Resources Bank (Sendai, Japan). These cells were cultured in Dulbecco's modified Eagle's medium (Huh-7, SKBR3, HeLa, KE-4, and SW480 cells), RPMI 1640 (A-549, WiDr, TE-8, and Lu65 cells) (SIGMA-ALDRICH, MO, USA), and Leibovitz's L15 (MDA-MB-231 cells) (Invitrogen) supplemented with 10% fetal bovine serum, MEM nonessential amino acids (Invitrogen), 200 unit/ml penicillin (Invitrogen), 200 µg/ml streptomycin (Invitrogen) and 2 mM L-glutamine (Invitrogen). MH-14 cells carrying the HCV subgenomic replicon [34] were cultured in the DMEM medium supplemented with 10% fetal bovine serum, MEM nonessential amino acids (Invitrogen), 200 unit/ml penicillin (Invitrogen), 200 µg/ml streptomycin (Invitrogen), 2 mM L-glutamine (Invitrogen) and 300 µg/ml G418 (Invitrogen). Five small interfering RNA (siRNA) duplexes containing 3′dTdT over

the hanging sequence were synthesized (Sigma-Aldrich, St. Louis, MO). These sequences were: si-1; 5′-GGACAUUCGCAUUGAUGAG-3′, si-2; 5′-CCUGUAAUUUGACUCAUAA-3′, si-3; 5′- GCCUUGGAUGUAAAUCUCUUU -3′, si-4; 5′- GGAGCUUUCAGUGACCAUA -3′, si-5; 5′-GGUCAAAUAAUAGUAGGAA-3′. A non-targeting siRNA (Sigma-Aldrich) was used as control. Plasmid and siRNA transfection was performed described previously [35]. In siRNA study, total RNAs from transfected cells were harvested after transfection for 5 days and examined mRNA copy number of CAHL by quantitative real-time RT-PCR.

Establishment of stable CAHL-knockdown cell by shRNA

Based on the siRNA data, we applied short hairpin RNA (shRNA) technology platform (Sigma Mission*RNAi*) to stably knockdown CAHL gene expression in MH14 cells. DNA oligo coding the effective siRNAs against each MH14-CAHL gene (5′-CCGGGCCTTGGATGTAAATCTCTTTCTCGAGAAAGAGATTTACATCCAAGGCTTTTTTG -3′) (sh-CAHL) was cloned into pLKO.1-puro shRNA vector. Plasmid DNA including non-targeting shRNA as control (sh-control) was transfected into MH14 cells along with Lentiviral Packaging Mix consisting of an envelope and packaging vector (Sigma-Aldrich) to produce lentivirus packed with shRNA cassettes using the standard procedure. After transfection, cells were cultured in the presence of 10 μg/ml puromycin.

Indirect immunofluorescence analysis

Anti-CAHL polyclonal antibody serum was generated in rabbits immunized with $CAHL_{1237\text{-}1251}$, ILHPKRGTEDRSDQS, according to our lab protocol [35]. Anti-NS3, NS4B, and NS5B, and NS5A were kindly provided from Dr. Kohara at The Tokyo Metropolitan Institute of Medical Science, Japan and Dr. Takamizawa at Osaka University, Japan, respectively. Cells were fixed with ice-cold acetone for 1 min, and then stained with anti-CAHL and anti-KDEL mAb (Santa Cruz Biotechnology, CA, USA) for ER antibodies followed by Alexa Fluor 488-conjugated goat anti-rabbit IgG and 594-conjugated goat anti-mouse IgG (Invitrogen), respectively, and visualized using a Bio-Rad MRC1024ES laser confocal scanning microscopy system (Bio-Rad Laboratories, CA, USA).

Immunoblot analysis

Immunoblot analysis was performed essentially as described previously [11,36].

RNA-protein binding precipitation assay

RNA-protein binding precipitation assay was essentially performed as described [11]. Briefly, to permeabilize plasma membrane, cells were treated 50 μg/ml digitonin (Nakarai Tesque Inc., Kyoto, Japan) in buffer B (20 mM HEPES-KOH [pH = 7.7], 110 mM KOAc, 2 mM MgOAc, 1 mM EGTA) at 25°C for 5 min. After treatment with 0.5 μg/ml proteinase K at 37°C for 5 min and washing with buffer B, cells were lysed in IP buffer (50 mM Tris-HCl [pH = 8], 150 mM NaCl, 0.5% NP-40, and protease inhibitory cocktail [Roche Applied Science]). After centrifugation, supernatants were incubated for 2 h with poly-U or protein G Sepharose resin (GE Healthcare). After four washes with IP buffer, precipitates were analyzed by immunoblot analysis. Supernatants after centrifugation were used as a positive control (designated Cell lysate in Fig. 4E and 4D).

GST-pull-down assay

GST-pull-down assay was performed as described previously [36].

Supporting Information

Figure S1 Predicted amino acid sequences of CAHL (NM_022828). Underlined residues (LLGQLRA) indicate identical sequence of phage clone #13.
(TIFF)

Figure S2 Indirect immunoflourescence analysis for colocalized with between CAHL and NS3, NS4A, NS4B, NS5A, and NS5B using Huh-7 (A) and MH-14 (B). The primary antibodies used were anti-CAHL (panels a, d, g, j, and m, green) and anti-NS proteins (panels b, e, h, k, and n, red) antibodies. Marge images of green and red signals are shown in panels c, f, i, l, and o.
(TIFF)

Figure S3 Determinant of knockdown efficiency against CAHL gene expression. Five siRNAs for the CAHL gene were individually transfected into MH-14 cells. After transfection, total RNAs of these cells were collected and examined mRNA copy number of CAHL by quantitative real-time RT-PCR.
(TIFF)

Table S1 List of phage clones and their encoding deduced peptide sequences screened by CsA biopanning. *Asterisk indicates the identical sequences.
(DOCX)

Author Contributions

Conceived and designed the experiments: KM HS KW K. Shimotohno SK K. Sakaguchi FS. Performed the experiments: KM HS KW KI TS KK KT HM AT. Analyzed the data: NS. Wrote the paper: KM HS KW FS.

References

1. Calne RY, White DJ, Thiru S, Evans DB, McMaster P, et al. (1978) Cyclosporin-A in patients receiving renal allografts from cadaver donors. Lancet 2: 1323–1327.
2. O'Keefe SJ, Tamura J, Kincaid RL, Tocci MJ, O'Neill EA (1992) FK-506- and CsA-sensitive activation of the interleukin-2 promoter by calcineurin. Nature 357: 692–694.
3. Clipstone NA, Crabtree GR (1992) Identification of calcineurin as a key signalling enzyme in T-lymphocyte activation. Nature 357: 695–697.
4. Liu J, Farmer JD, Jr., Lane WS, Friedman J, Weissman I, et al. (1991) Calcineurin is a common target of cyclophilin-cyclosporin A and FKBP-FK506 complexes. Cell 66: 807–815.
5. Fruman DA, Klee CB, Bierer BE, Burakoff SJ (1992) Calcineurin phosphatase activity in T lymphocytes is inhibited by FK 506 and cyclosporin A. Proc Natl Acad Sci U S A 89: 3686–3690.
6. Fischer G, Tradler T, Zarnt T (1998) The mode of action of peptidylprolyl cis/trans isomerases *in vivo*: binding vs. catalysis. FEBS Lett 426: 17–20.
7. Braaten D, Luban J (2001) Cyclophilin A regulates HIV-1 infectivity, as demonstrated by gene targeting in human T cells. EMBO J 20: 1300–1309.
8. Waldmeier PC, Zimmermann K, Qian T, Tintelnot-Blomley M, Lemasters JJ (2003) Cyclophilin D as a drug target. Curr Med Chem 10: 1485–1506.
9. Hanoulle X, Badillo A, Wieruszeski JM, Verdegem D, Landrieu I, et al. (2009) Hepatitis C virus NS5A protein is a substrate for the peptidyl-prolyl cis/trans isomerase activity of cyclophilins A and B. J Biol Chem 284: 13589–13601.
10. Liu Z, Yang F, Robotham JM, Tang H (2009) Critical role of cyclophilin A and its prolyl-peptidyl isomerase activity in the structure and function of the hepatitis C virus replication complex. J Virol 83: 6554–6565.
11. Watashi K, Ishii N, Hijikata M, Inoue D, Murata T, et al. (2005) Cyclophilin B is a functional regulator of hepatitis C virus RNA polymerase. Mol Cell 19: 111–122.
12. Kuramochi K, Haruyama T, Takeuchi R, Sunoki T, Watanabe M, et al. (2005) Affinity capture of a mammalian DNA polymerase beta by inhibitors immobilized to resins used in solid-phase organic synthesis. Bioconjug Chem 16: 97–104.

13. Aoki S, Morohashi K, Sunoki T, Kuramochi K, Kobayashi S, et al. (2007) Screening of paclitaxel-binding molecules from a library of random peptides displayed on T7 phage particles using paclitaxel-photoimmobilized resin. Bioconjug Chem 18: 1981–1986.
14. Smith GP, Petrenko VA (1997) Phage Display. Chem Rev 97: 391–410.
15. Rodi DJ, Soares AS, Makowski L (2002) Quantitative assessment of peptide sequence diversity in M13 combinatorial peptide phage display libraries. J Mol Biol 322: 1039–1052.
16. Mandava S, Makowski L, Devarapalli S, Uzubell J, Rodi DJ (2004) RELIC–a bioinformatics server for combinatorial peptide analysis and identification of protein-ligand interaction sites. Proteomics 4: 1439–1460.
17. Rodi DJ, Mandava S, Makowski L (2004) DIVAA: analysis of amino acid diversity in multiple aligned protein sequences. Bioinformatics 20: 3481–3489.
18. Makowski L, Rodi DJ (2003) Genome-wide characterisation of the binding repertoire of small molecule drugs. Hum Genomics 1: 41–51.
19. Aoki S, Ohta K, Yamazaki T, Sugawara F, Sakaguchi K (2005) Mammalian mitotic centromere-associated kinesin (MCAK): a new molecular target of sulfoquinovosylacylglycerols novel antitumor and immunosuppressive agents. FEBS J 272: 2132–2140.
20. Morohashi K, Yoshino A, Yoshimori A, Saito S, Tanuma S, et al. (2005) Identification of a drug target motif: an anti-tumor drug NK109 interacts with a PNxxxxP. Biochem Pharmacol 70: 37–46.
21. Kanoh N, Honda K, Simizu S, Muroi M, Osada H (2005) Photo-cross-linked small-molecule affinity matrix for facilitating forward and reverse chemical genetics. Angew Chem Int Ed Engl 44: 3559–3562.
22. Loor F, Tiberghien F, Wenandy T, Didier A, Traber R (2002) Cyclosporin: structure-activity relationships for the inhibition of the human FPR1 formyl peptide receptor. J Med Chem 45: 4613–4628.
23. Yang F, Robotham JM, Nelson HB, Irsigler A, Kenworthy R, et al. (2008) Cyclophilin A is an essential cofactor for hepatitis C virus infection and the principal mediator of cyclosporine resistance in vitro. J Virol 82: 5269–5278.
24. Chatterji U, Bobardt M, Selvarajah S, Yang F, Tang H, et al. (2009) The isomerase active site of cyclophilin A is critical for hepatitis C virus replication. J Biol Chem 284: 16998–17005.
25. Fernandes F, Poole DS, Hoover S, Middleton R, Andrei AC, et al. (2007) Sensitivity of hepatitis C virus to cyclosporine A depends on nonstructural proteins NS5A and NS5B. Hepatology 46: 1026–1033.
26. Robida JM, Nelson HB, Liu Z, Tang H (2007) Characterization of hepatitis C virus subgenomic replicon resistance to cyclosporine in vitro. J Virol 81: 5829–5840.
27. Bouchard R, Bailly A, Blakeslee JJ, Oehring SC, Vincenzetti V, et al. (2006) Immunophilin-like TWISTED DWARF1 modulates auxin efflux activities of Arabidopsis P-glycoproteins. J Biol Chem 281: 30603–30612.
28. Flisiak R, Feinman SV, Jablkowski M, Horban A, Kryczka W, et al. (2009) The cyclophilin inhibitor Debio 025 combined with PEG IFNalpha2a significantly reduces viral load in treatment-naïve hepatitis C patients. Hepatology 49: 1460–1468.
29. Ariumi Y, Kuroki M, Abe K, Dansako H, Ikeda M, et al. (2007) DDX3 DEAD-box RNA helicase is required for hepatitis C virus RNA replication. J Virol 81: 13922–13926.
30. Jangra RK, Yi M, Lemon SM (2010) Regulation of hepatitis C virus translation and infectious virus production by the microRNA miR-122. J Virol 84: 6615–6625.
31. Goh PY, Tan YJ, Lim SP, Tan YH, Lim SG, et al. (2004) Cellular RNA helicase p68 relocalization and interaction with the hepatitis C virus (HCV) NS5B protein and the potential role of p68 in HCV RNA replication. J Virol 78: 5288–5298.
32. Larrea E, Garcia N, Qian C, Civera MP, Prieto J (1996) Tumor necrosis factor a gene expression and the response to interferon in chronic hepatitis C. Hepatology 23: 210–217.
33. Okanami M, Meshi T, Iwabuchi M (1998) Characterization of a DEAD box ATPase/RNA helicase protein of *Arabidopsis thaliana*. Nucleic Acids Res 26: 2638–2643.
34. Watashi K, Hijikata M, Hosaka M, Yamaji M, Shimotohno K (2003) Cyclosporin A suppresses replication of hepatitis C virus genome in cultured hepatocytes. Hepatology 38: 1282–1288.
35. Imai A, Sahara H, Tamura Y, Jimbow K, Saito T, et al. (2007) Inhibition of endogenous MHC class II-restricted antigen presentation by tacrolimus (FK506) via FKBP51. Eur J Immunol 37: 1730–1738.
36. Watashi K, Hijikata M, Tagawa A, Doi T, Marusawa H, et al. (2003) Modulation of retinoid signaling by a cytoplasmic viral protein via sequestration of Sp110b, a potent transcriptional corepressor of retinoic acid receptor, from the nucleus. Mol Cell Biol 23: 7498–7509.

Available online at www.sciencedirect.com
ScienceDirect
Current Opinion in Virology

Lipoprotein component associated with hepatitis C virus is essential for virus infectivity

Yuko Shimizu[1,3], Takayuki Hishiki[1,3], Saneyuki Ujino[1], Kazuo Sugiyama[2], Kenji Funami[1] and Kunitada Shimotohno[1]

Many chronic hepatitis patients with hepatitis C virus (HCV) are observed to have a degree of steatosis which is a factor in the progression of liver diseases. Transgenic mice expressing HCV core protein develop liver steatosis before the onset of hepatocellular carcinoma, suggesting active involvement of HCV in the de-regulation of lipid metabolism in host cells. However, the role of lipid metabolism in HCV life cycle has not been fully understood until the establishment of *in vitro* HCV infection and replication system.In this review we focus on HCV production with regard to modification of lipid metabolism observed in an *in vitro* HCV infection and replication system. The importance of lipid droplet to HCV production has been recognized, possibly at the stage of virus assembly, although the precise mechanism of lipid droplet for virus production remains elusive. Association of lipoprotein with HCV in circulating blood in chronic hepatitis C patients is observed. In fact, HCV released from culture medium is also associated with lipoprotein. The fact that treatment of HCV fraction with lipoprotein lipase (LPL) abolished infectivity indicates the essential role of lipoprotein's association with virus particle in the virus life cycle. In particular, apolipoprotein E (ApoE), a component of lipoprotein associated with HCV plays a pivotal role in HCV infectivity by functioning as a virus ligand to lipoprotein receptor that also functions as HCV receptor. These results strongly suggest the direct involvement of lipid metabolism in the regulation of the HCV life cycle.

Addresses
[1] Research Institute, Chiba Institute of Technology, Tsudanuma, Narashino, Chiba 275-0016, Japan
[2] Center for Integrated Medical Research, Keio University, Shinjuku-ku, Shinanomachi 35, Tokyo 160-8582, Japan

Corresponding author: Shimotohno, Kunitada (kunitada.shimotono@it-chiba.ac.jp)
[3] These authors contributed equally.

Current Opinion in Virology 2011, **1**:19–26

This review comes from a themed issue on
Virus Entry
Edited by François-Loïc Cosset and Urs Greber

Available online 12th June 2011

1879-6257/$ – see front matter

DOI 10.1016/j.coviro.2011.05.017

Introduction

Infection with hepatitis C virus (HCV), which persists with a rate of up to 80% and is difficult to eliminate, is estimated to occur in about 3% of the world population [1]. HCV infection frequently causes chronic hepatitis, which often leads to the development of liver cirrhosis and hepatocellular carcinoma after a long latency period [2]. The combined therapy of ribavirin and interferon is currently a major treatment to infected patients, although half of them have experienced the benefit of this treatment along with a severe side effect. Therefore, clarification of the underlying molecular mechanism of HCV life cycle is necessary for the development of a new effective therapy.

The progression of liver disease in patients with HCV is thought to result from a persistent inflammation accompanied by periportal necrosis and fibrosis [3]. Many chronic hepatitis patients with HCV, but not with HBV, are also noted to have a degree of steatosis by the examination of their liver biopsies [4]. Hepatic steatosis is defined as excessive lipid accumulation/infiltration within the hepatocyte, and has recently been recognized as an important cause for cirrhosis [5]. It seems likely that hepatic steatosis in chronic hepatitis C patients is somehow related to HCV infection and its replication. Furthermore, the combination of steatosis and the presence of HCV has been associated with a more rapid progression of fibrosis. Although the precise mechanism of how HCV infection results in the accumulation of excessive lipid levels and causes hepatocyte steatosis remains elusive, increasing evidence strongly suggests that HCV-encoded protein(s) plays some roles in this process.

HCV, which belongs to the family *Flaviviridae*, has a 9.6-kb positive single strand of RNA as a genome. The HCV RNA is translated into a precursor polyprotein that is processed concertedly with translation, or after the translation by cleavage with cellular and viral proteases to produce about 10 viral proteins, structural proteins (core, E1, and E2), and nonstructural proteins (p7, NS2, NS3, NS4A, NS4B, NS5A, and NS5B). With the help of nonstructural proteins, viral replication occurs in the endoplasmic reticulum (ER) membranous structure. In this review, we discuss the effect of HCV infection on host lipid metabolism and transfer, as well as the early event of virus entry required for HCV life cycle.

Regulation of lipid metabolism by HCV proteins

Expression of HCV core as well as the complete HCV genome in some transgenic mice induces steatosis [6,7]. It is notable to observe the association of HCV core with the